THE PARKES CATALOGUE OF RADIO SOURCES DECLINATION ZONE −20° TO −60°

By J. G. Bolton,* F. F. Gardner,* and M. B. Mackey*

[*Manuscript received April* 9, 1964]

Summary

A catalogue of 297 radio sources between declinations −20° and −60° has been compiled from observations with the Australian 210-ft telescope. The sources were selected from a survey at 75 cm wavelength as having flux densities in excess of 4×10^{-26} W $m^{-2}(c/s)^{-1}$. The survey did not cover a small area near the galactic plane. Additional measurements were made at wavelengths of 21 and 11 cm. Results on source identification, spectra, and polarization are discussed.

I. Introduction

This paper contains the results of the first part of a survey for radio sources between declinations +20° and −90° being made with the 210-ft reflector of the Australian National Radio Astronomy Observatory at Parkes, New South Wales. The survey is in four zones, of which observations are complete for declinations −20° to −60° and −60° to −90°, almost complete for +20° to 0°, and in progress for 0° to −20°. Some areas near the galactic plane are not covered in this survey but are the subject of a separate investigation. The catalogue is being compiled to provide a basic list of the more intense sources for subsequent detailed measurements of parameters such as precise position, brightness distribution, spectrum, and polarization. Although such a catalogue for the southern hemisphere already exists (Mills, Slee, and Hill 1958, 1960, 1961)—subsequently referred to as MSH—it was felt advisable to repeat this work for the following reasons.

(1) The wavelengths at which the 210-ft telescope can be used to the greatest advantage are considerably shorter than that of the MSH survey.

(2) More accurate positions than those in the MSH catalogue are desirable for observations with a narrow pencil-beam instrument.

(3) There are some discrepancies between the MSH catalogue and other observations (Kellermann and Harris 1960; Bennett and Smith 1961).

The observations consisted of an initial finding survey at a wavelength of 75 cm, measurements of flux densities and positions at 21 cm, measurements of flux densities and positions at 11 cm, and determination of the polarization of the 63 most intense sources at 21 cm. The flux density scales have been adopted to agree with those in the recent compilation of source spectra by Conway, Kellermann, and Long (1963)—subsequently referred to as CKL. The position calibration of the 210-ft telescope is discussed in some detail. Positions of about one-third of the sources have been examined on Palomar Sky Survey prints, or plates made with the 74-in. Mount Stromlo reflector. Log N–log S counts are presented at the three

* Division of Radiophysics, CSIRO, University Grounds, Chippendale, N.S.W.

survey wavelengths, and also at 350 cm. Spectra of sources and the relation between polarization and spectral characteristics are discussed. Finally, differences between the present results and the MSH survey are investigated.

II. The Basic Survey at 75 cm

The basic survey was made at the nominal wavelength of 75 cm (actually 408 Mc/s) where the beamwidth of the telescope is 48′ of arc. The receiver, constructed by F. Tonking (Mackey 1964), has a double-sideband crystal mixer with an input temperature of about 300°K and a bandwidth of 8 Mc/s. The receiver is switched between the aerial feed and a reference load at liquid nitrogen temperature.

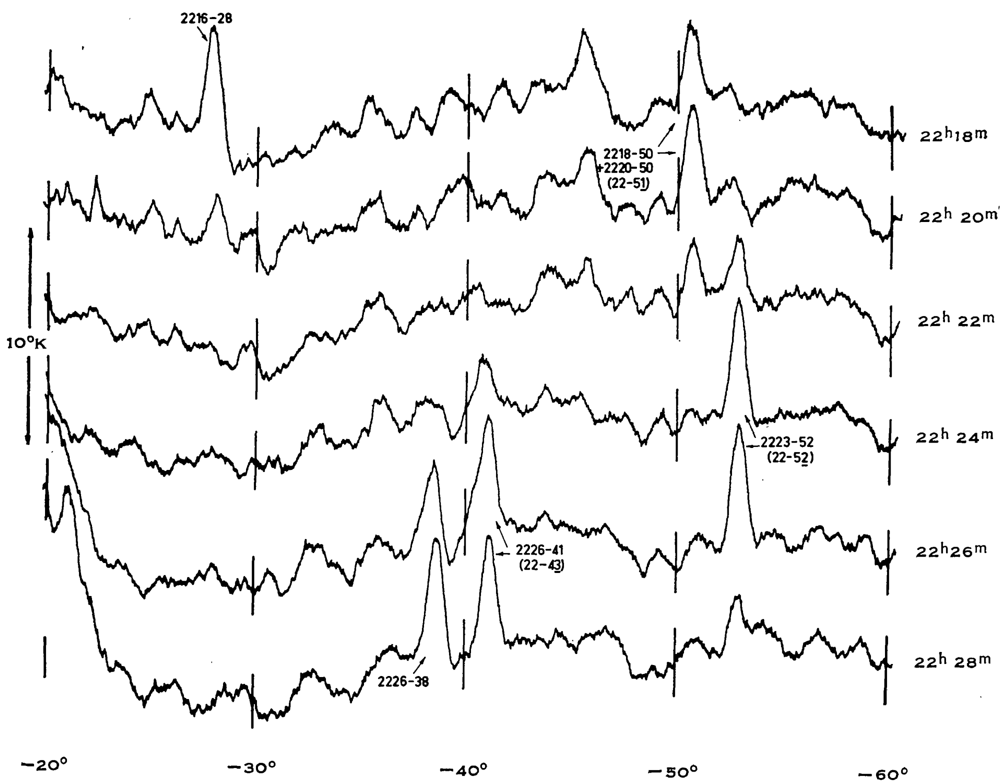

Fig. 1(*a*).—Facsimilies of five adjacent declination scans at 75 cm from the finding survey. The five sources identified on the records are included in the catalogue.

With a 2-second time-constant, peak-to-peak noise fluctuations are about 0·5°K. At the maximum drive rate of the telescope in equatorial coordinates of $2\frac{1}{2}$°/min, the time to traverse the beam width is 20 s, or 10 times the chosen time-constant. Even at the maximum drive rate, used throughout the 75-cm survey, the sensitivity of the instrument was limited by confusion effects due to faint sources and variations in background radiation rather than by system noise.

The observational procedure was to make a series of scans in declination at intervals of 2 min in right ascension. These scans were therefore 28′ apart at −20°

declination and 15′ apart at −60° declination. From the records of these scans objects were selected which were ⩾ 2·5°K in aerial temperature (∼ 4×10^{-26} W $m^{-2}(c/s)^{-1}$) and which were not noticeably broader than the aerial beam in either coordinate. The survey was principally aimed at extragalactic objects, only a few of which have diameters in excess of 20′ of arc, necessary to produce such broadening.

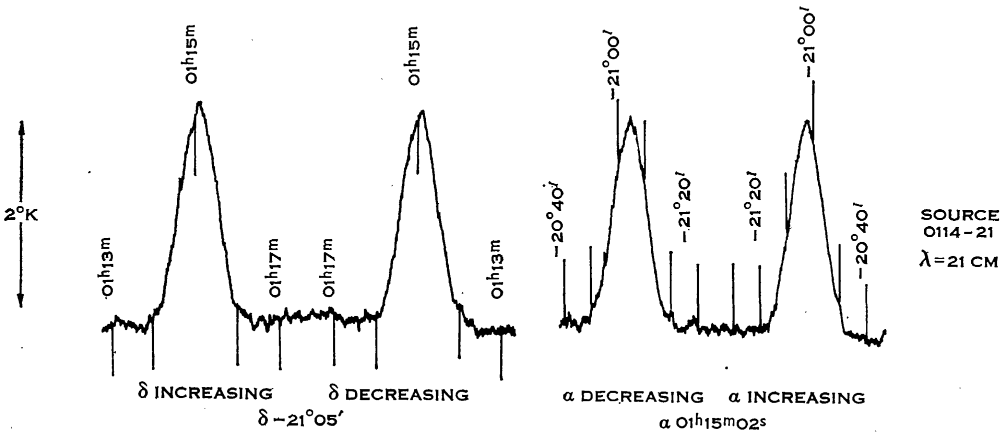

Fig. 1(*b*).—Examples of a 21-cm record comprising forward and reverse scans in right ascension and declination. Position markers are at intervals of 1 min in R.A. and 10′ in declination.

The value of the declination of a source could be determined fairly precisely from individual scans and an estimate of the right ascension was made from comparison of amplitudes on adjacent scans. Figure 1(*a*) contains facsimiles of the 75-cm survey scans for right ascensions 22^{h} 18^{m} to 22^{h} 28^{m}. Five sources indicated in this figure are included in the catalogue. They comprise three sources previously catalogued

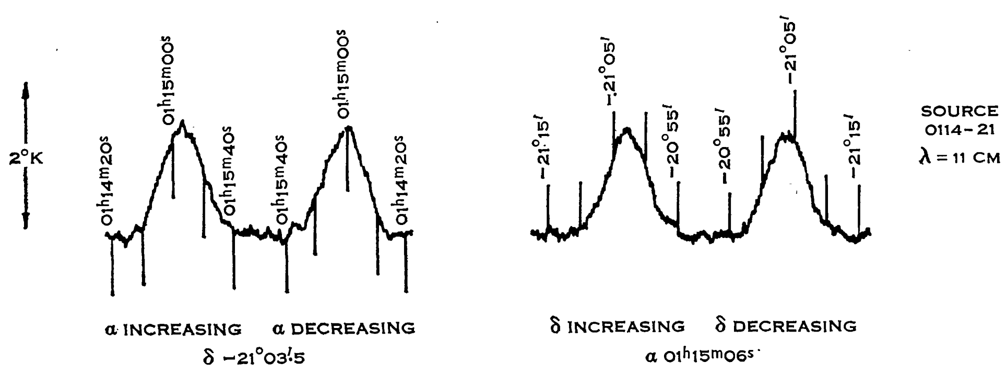

Fig. 1(*c*).—Examples of an 11-cm record comprising forward and reverse scans in right ascension and declination. Position markers are at intervals of 20 s in R.A. and 5′ in declination.

by Mills, Slee, and Hill (one of which, 22−*51*, is resolved into a double at 21 cm) and two not previously catalogued. The 75-cm survey was discontinued near the galactic plane wherever the aerial temperature due to background is more than ∼ 20°K above the regions of minimum temperature in the survey area. The area covered in the finding survey is approximately 2·7 steradians; the region not covered is shown in Figure 2.

III. The 21-cm Observations

All the sources selected from the 75-cm survey were re-observed at a nominal wavelength of 21 cm (actually 1410 Mc/s). The feed system permitted simultaneous observation at both 75 and 21 cm. The 21-cm receiver (Gardner and Milne 1963), a degenerate parametric with a 10 Mc/s bandwidth and system temperature of 100°K, has peak-to-peak noise fluctuations of only 0·15°K with the 2-second output time-constant used in the observations. In this receiver a backward-looking sky horn is used as the reference element.

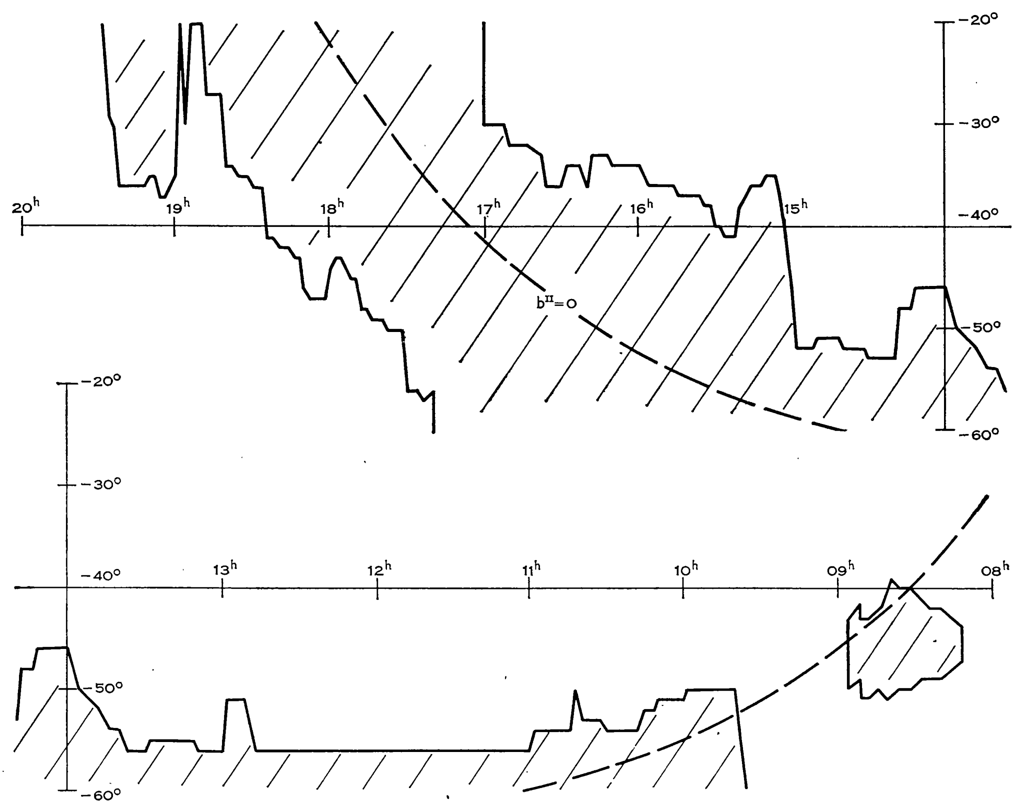

Fig. 2.—The region of the sky between declinations −20° and −60° which is not covered in the present survey. Hatched area is the excluded region. The dashed line indicates the new galactic equator.

The observational procedure was to set the telescope on the position found at 75 cm and about 0·5° away from the approximate right ascension. It was then scanned past the source at a rate of $\sim 2^{\rm m} \times \sec \delta$ per minute. From drives in both directions an improved value of right ascension was found. With this right ascension, declination scans were made across the source at 0·5°/min and a more accurate value of declination was obtained. If the new value of declination differed by more than 5′ from the 75-cm value, repeat right ascension scans were made at the revised declination. Examples of 21-cm records are shown in Figure 1(*b*). Finally, a right ascension scan, several degrees in extent, was made through the source;

this observation combined with the survey scans in declination was used to estimate the 75-cm flux density.

The 21-cm observations showed that some 5–10% of the sources selected from the 75-cm survey were probably background variations and these were rejected from the catalogue. Twelve of the sources were clearly resolved into two objects of the same order of intensity. Their significance as physical or non-physical doubles is discussed later.

IV. The 11-cm Observations

All the sources in the 21-cm list were observed again at 11 cm (2650 Mc/s) using the same procedure as at 20 cm. However, the declination and right ascension scan rates were carefully set to values of $0\cdot25°$ and $1^{m}\times\sec\delta$ per minute so that beam broadening, and thus angular size effects, could be easily detected. The 11-cm receiver is of the degenerate parametric type (Cooper, Cousins, and Gruner 1964) and switches between the aerial feed and a sky horn reference. The overall system temperature is $\sim 150°$K and the i.f. bandwidth about 40 Mc/s. With a 2-second output time-constant as used in these observations peak-to-peak noise fluctuations are $\sim 0\cdot15°$K. Most of the sources measured had aerial temperatures in excess of $0\cdot4°$K. A typical 11-cm record is shown in Figure 1(*c*).

The 11-cm observations provided an independent check on numerical errors in the reduction of the 21-cm positions. One component of a source found to be double at 21 cm was further resolved into two sources. Beam broadening, indicating source sizes of the order of 3′ of arc or greater, was detected in a further 20 cases.

V. Polarization Observations at 21 cm

Sixty-three of the most intense sources were examined for linear polarization at 21 cm using techniques previously described by Gardner and Whiteoak (1962). The measurements were made with a special single-wavelength feed equipped with a rotating coaxial joint. No polarization was detected for 15 sources; polarization in excess of 2% was found for 28 sources, of which 11 were polarized in excess of 5%. Only the percentage polarization is reported in this catalogue; a full investigation of polarization characteristics such as position angle, dependence on wavelength, and Faraday rotation is being made by F. F. Gardner and R. D. Davies and will be published separately.

The 210-ft telescope is on an altazimuth mounting and thus the position angle of the feed changes with hour angle and declination. The position and intensity measurements were made without regard to changes in position angle. For sources not specifically investigated for polarization, possible linear polarization represents a source of error in the flux density measurements; however, the average error from this cause is probably only of the order of 1 or 2%.

VI. Determination of Flux Densities

Conway, Kellermann, and Long (1963) have recently rationalized the flux density scales in use at observatories in the northern hemisphere. Rather than use independent calibration in this work we have attempted to adopt the same scales through observation of a number of sources in the CKL list. Receiver calibration for each observation was made by injecting a known noise signal from a discharge lamp through a directional coupler into the line between the aerial feed and the r.f. switch. The values of these signals, against which the aerial

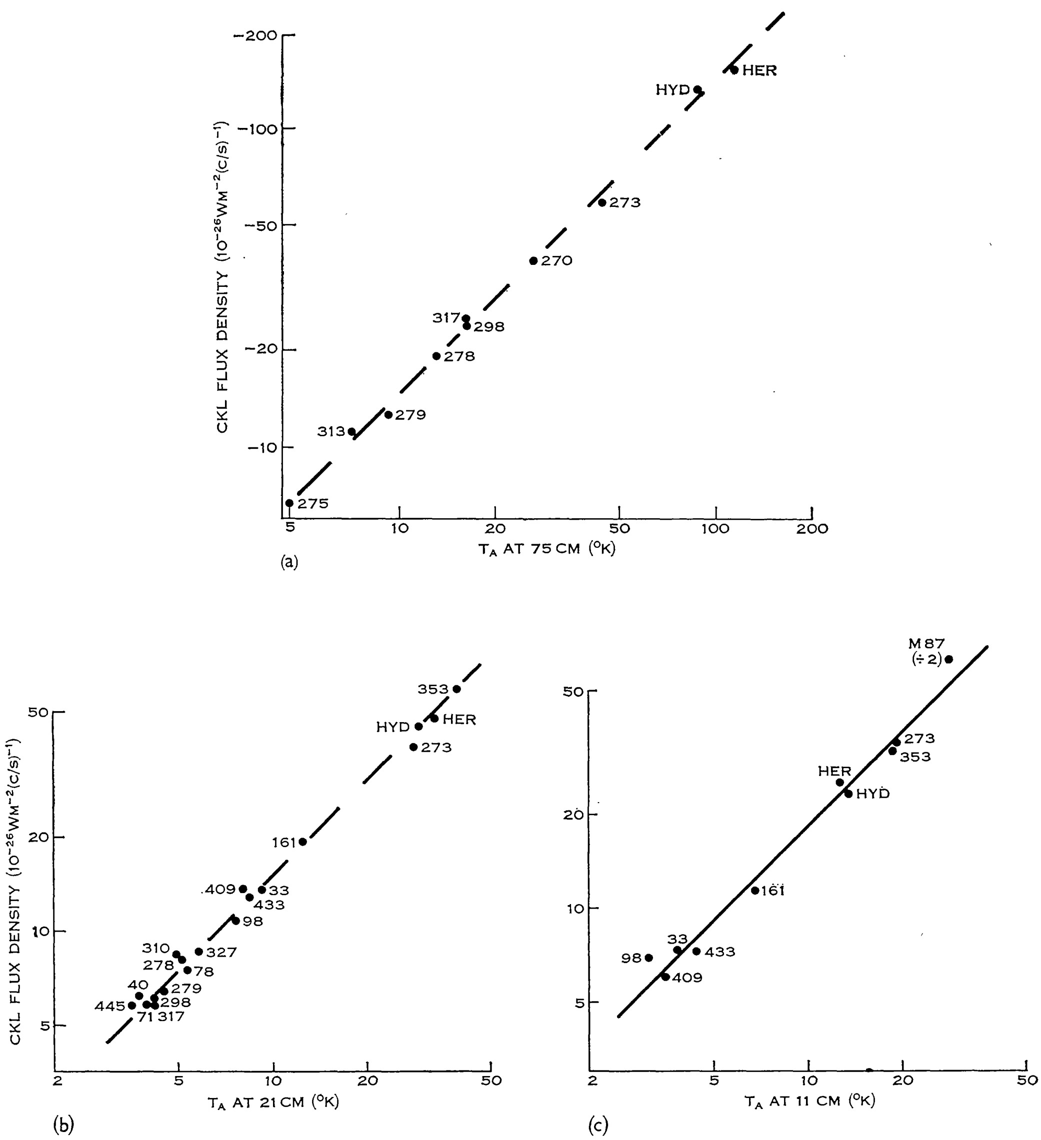

Fig. 3.—Comparison between flux densities of sources from measurements by Conway, Kellermann, and Long (CKL) and observed aerial temperatures for the 210-ft telescope. (*a*) 75 cm, (*b*) 21 cm, and (*c*) 11 cm.

temperature due to a source was measured, were calibrated by B. F. C. Cooper against more fundamental standards. Figure 3 shows the relation between CKL flux densities and apparent aerial temperatures of the 210-ft telescope. At 75 cm

(Fig. 3(*a*)) the CKL values from column 13 of their table were used. These had been determined from the best fitting curve to all points in the range from 20 to 870 cm.

Similarly, at 21 and 11 cm (Figs. 3(*b*) and 3(*c*)) we have read off values from the curves of best fit in the range from 10 to 40 cm. The multiplying factors to convert from the 210-ft aerial temperatures to flux densities on the CKL scales are 1·47, 1·55, and 1·80 at 75, 21, and 11 cm respectively. These imply corresponding aerial efficiencies of 58, 55, and 47% for the feeds in question. This variation in efficiency with wavelength is consistent with an r.m.s. deviation of 4–5 mm in surface accuracy deduced from direct survey measurements of the basic structure and measurements of individual skin panels (Bowen and Minnett 1962). The factor of 1·55 at 21 cm refers to the single-wavelength feed used for polarization and intensity comparison measurements. For the dual 75–21 cm feed used in most of the survey work the conversion factor is 6% higher and the aerial efficiency correspondingly lower.

Having decided on relative scales of flux density, we have to consider the reliability of the individual measurements with respect to these scales. There are two types of error, those that are proportional to the flux density, arising from scaling factors, and those that are fixed in flux density. The latter comprise errors from noise fluctuations and confusion effects. The average error from noise fluctuations, when the mean of four scans through the source is used, is not likely to exceed half the peak-to-peak fluctuations. At 11 and 21 cm this corresponds to 0·1 flux units. At 75 cm, where only two scans were used, it is about 0·5 f.u. Confusion errors are negligible at the short wavelengths but can be quite severe at 75 cm. The average difference between flux densities judged from scans in declination and right ascension is about 1 f.u., which is of the same order as the background variations shown in the records of Figure 1(*a*). The average error from this cause would be about 0·5 f.u., especially if one takes account of possible polarization of the background.

The proportional errors comprise errors due to variations in calibration signal—or aerial gain, unknown polarization, and angular extent. Repeated observations on strong sources during the survey work revealed differences in their aerial temperatures in terms of the calibration signal of up to $\pm 5\%$. The exact cause of this is not known. As pointed out in the previous section, unknown polarization of the weaker sources could result in errors as high as 15% at 11 or 21 cm in an extreme case, but the average would be only 1 or 2%. At 75 cm errors from this cause are negligible. Sources $\geqslant 3'$ of arc in angular diameter show noticeable beam broadening at 11 cm. These are indicated in the "remarks" column of the catalogue. Except where specially stated, the values of flux are the peak values on the records and thus represent lower limits. Sources below $2'$ of arc have negligible errors in their estimate of flux density due to resolution. However, weak sources between $2'$ and $3'$ of arc, whose broadening could not be detected, could be underestimated by 7–16% at 11 cm and 2–5% at 21 cm. From available statistics on the diameters of sources, we would expect 15–20% of sources to be in this range.

When both the fixed and proportional effects are combined the following estimates of average and extreme errors result:

λ (cm)	Average Error	Extreme Error
11	±0·07 f.u. ±7%	±0·17 f.u. ±21%
21	±0·05 f.u. ±6%	±0·15 f.u. ±12%
75	±0·6 f.u. ±5%	±1·6 f.u. ±5%

At the level of flux density exceeded by 70% of the catalogued sources (the approximate turnover point in the $\log N$–$\log S$ curve of Section X), the corresponding values would be:

λ (cm)	Flux Density	Average Error	Extreme Error
11	1	±0·14	±0·38
21	2	±0·17	±0·39
75	5	±0·9	±1·9

VII. Position Calibration

The period of this survey has also been the period in which the pointing errors in the 210-ft telescope have been evaluated and to a large extent overcome. The evaluation of these errors has depended in part on the observation of radio sources of known or assumed known position. Near the northern limit of the telescope, sources whose positions have been determined precisely by the Caltech and Cambridge observatories have been used as calibrators. In the southern hemisphere there are no such calibrators. One of the reasons for this survey was to obtain southern identifications (see Section IX), some of which have been used in the calibration program.

The overall pointing calibration program has been directed by Dr. J. A. Roberts, who has been responsible for many of the observations and nearly all the evaluation. Subsequent adjustments to the telescope have been made by Mr. A. J. Shimmins. As the basic axes of the telescope are altazimuth and those of the master control system equatorial (Bowen and Minnett 1962), pointing errors occur in both coordinate systems.

Errors in the master equatorial arise from misalignment of the polar axis and deflections in its structure.

The polar axis was originally set during construction to within 15″ of the correct azimuth and zenith angle. Subsequent checks have been made by observing the apparent positions of FK3 stars both near the pole and in the general field. These observations showed that the master equatorial, which is independently mounted on a part-steel, part-concrete column 80 ft high, is stable over long periods of time. The initial azimuth and zenith angle errors have been reduced, in a series of adjustments, to only a few seconds of arc. It is believed that within ±4 hr hour angle, the master equatorial pointing errors are now comparable to the last digit in the readout indicators (1^s in R.A., 0·1′ in declination).

Table 1

SOURCE CATALOGUE

Catalogue Number	Position (1950)		Annual Precession		Flux Density				Spectrum			Remarks	Galactic Coordinates		MSH Cat. No.
	R.A.	δ	Δα	+Δδ	350	75	21	11	75→350	21→75	11→21	(Ang. Size, Identification, etc.)	l^{II}	b^{II}	
0003−56	00 03 20	−56 45·8	3·04	20·04	19	6·1	2·0	1·1	0·7	0·9	0·9		316	−60	00−*51*
0003−42	00 03 28	−42 52·3	3·05	20·04	17	4·6	1·7	0·9	0·8	0·8	1·0		332	−72	00−*42*
0007−44	00 07 58	−44 40·0	3·01	20·02	31	6·5	1·7	0·9	1·0	1·1	1·0	~1′NS	326	−71	00−*43*
0008−42	00 08 22	−42 10·2	3·02	20·02		6·4	5·4	2·6		0·1	1·1	P0·2%	330	−73	
0012−38	00 12 52	−38 21·1	3·01	20·01	19	4·9	1·6	0·7	0·9	0·9	1·3		336	−77	00−*35*
0020−25	00 20 38	−25 19·3	3·02	19·96	21	4·8	2·4	1·4	0·9	0·6	0·8	>1′NS III	52	−83	00−*27*
0021−29	00 21 58	−29 45·7	2·99	19·96	33	8·2	3·3	1·6	0·9	0·7	1·2	~20″EW III	13	−84	00−*29*
0023−33	00 23 02	−33 20·1	2·99	19·95	20	5·9	1·7	0·8	0·8	1·0	1·2	>1′NS 74I	346	−82	00−*38*
0023−26	00 23 18	−26 18·8	3·01	19·93	17	20	9·0	5·8	−0·1	0·6	0·7	III P1·8%	45	−84	00−*210*
0032−20	00 32 39	−20 20·7	3·00	19·84	19	5·9	2·4	1·0	0·7	0·7	1·4	III	95	−82	00−*216*
0035−39	00 35 59	−39 16·5	2·90	19·79	30	5·8	1·9	0·9	1·0	0·9	1·2	15″EW	315	−78	00−*313*
0039−44	00 39 46	−44 30·8	2·85	19·73	35	12	4·3	2·1	0·7	0·8	1·1	<15″EW	308	−73	00−*410*
0042−35	00 42 15	−35 47·1	2·90	19·70	13	5·9	3·1	1·6	0·5	0·5	1·0		312	−82	00−*315*
0043−42	00 43 52	−42 24·3	2·84	19·67	52	21	9·1	5·0	0·6	0·7	1·0	>1′NS 40″EW 74II P8·8%	306	−75	00−*411*
0045−25	00 45 06	−25 33·4	2·94	19·66	29	15	6·3	3·6	0·4	0·7	0·9	NGC 253 7·0mag.Sc P<1·5%	96	−88	00−*222*
0048−44	00 48 25	−44 45·1	2·80	19·58	16	4·2	1·6	0·7	0·9	0·8	1·3		304	−73	00−*413*
0049−43	00 49 52	−43 23·3	2·83	19·56	23	7·3	3·4	1·6	0·7	0·6	1·2		302	−74	00−*414*
0103−45	01 03 06	−45 22·0	2·70	19·29	41	7·5	2·8	1·5	1·1	0·8	1·0	23″EW	295	−72	01−*41*
0114−47	01 14 05	−47 38·1	2·60	18·99	34	10·4	2·1	0·8	0·8			>40″EW ext in δ at 11 cm, may be double	291	−61	01−*45*
0114−21	01 14 26	−21 07·7	2·91	18·98	18	11·6	4·1	1·9	0·3	0·8	1·2	<20″NS P0·6%	166	−81	01−*26*
0119−37	01 19 45	−37 46·9	2·70	18·82	19	4·9	1·2	0·6	0·9	1·0	1·1		272	−78	01−*38*
0122−25	01 22 26	−25 33·6	2·85	18·74	9	4·2	1·3	0·7	0·5	0·9	1·0	II	200	−82	01−*29*
0124−40	01 24 12	−40 59·1	2·64	18·69	33	6·4	1·4	0·6			1·4		277	−75	01−*48*
0125−41	01 25 02	−41 28·2	2·64	18·69			1·4	0·7			1·1	74III	277	−74	

0126−53	01 26 29	−53 10·4	2·41	18·61	11	3·8	0·9	0·6	0·7	1·2	0·6		290	−63	01−*54*
0128−26	01 28 07	−26 25·5	2·82	18·56	18	5·7	1·2	0·6	0·7	1·2	1·1	<20″NS	207	−81	01−*211*
0129−51	01 29 11	−51 18·5	2·44	18·52	8	3·1	1·0	0·5	0·6	0·9	1·1		288	−65	01−*55*
0131−44	01 31 24	−44 59·4	2·54	18·45	18	5·9	2·1	1·2	0·7	0·9	0·8	P11%	280	−70	01−*49*
0131−36	01 31 42	−36 44·6	2·68	18·44	56	16	7·1	3·4	0·8	0·7		>45″EW 74I 15mag.EO ext at 11 cm	261	−77	01−*311*
0148−29	01 48 20	−29 46·5	2·72	17·80	63	12·8	2·8	1·8			0·7	>1′NS?	226	−77	01−*217*
0149−29	01 49 53	−29 54·5	2·72	17·75			1·1	0·7			0·7	<20″NS? III	228	−76	
0157−31	01 57 57	−31 08·2	2·67	17·42	26	9·3	3·7	2·4	0·7	0·7	0·7	<15″EW ∼30″NS II P3%	230	−74	01−*315*
0201−44	02 01 40	−44 03·9	2·41	17·26	9	5·7	2·8	1·8	0·3	0·6	0·7		266	−68	02−*41*
0211−34	02 11 07	−34 27·2	2·58	16·82	13	4·4	0·8	0·5	0·7		0·7	ext to N or 2nd source at 21 cm	239	−71	02−*32*
0214−48	02 14 53	−48 03·4	2·25	16·64	31	9·5	2·4	1·3	0·8	1·1	1·0	>40″EW	270	−63	02−*43*
0216−25	02 16 29	−25 03·1	2·71	16·56	15	4·7	1·3	0·7	0·7	1·1	1·0	III	211	−70	02−*25*
0216−36	02 16 56	−36 40·1	2·50	16·54	29	7·1	1·4	0·7	0·9	1·3	1·1	>40″EW	245	−69	02−*33*
0220−42	02 20 21	−42 13·9	2·33	16·37	17	4·2	0·9	1·6	0·9	1·2	0·3		257	−66	02−*45*
0221−28	02 21 29	−28 32·5	2·65	16·31	11	4·3	1·3	0·6	0·6	1·0	1·2	III	221	−70	02−*26*
0222−23	02 22 49	−23 26·3	2·73	16·24	19	6·2	1·8	1·1	0·7	1·0	0·8	<20″NS III	208	−68	02−*27*
0228−39	02 28 54	−39 57·3	2·40	15·92		5·2	1·2	0·7		1·2	0·9		251	−65	
0231−23	02 31 07	−23 33·7	2·72	15·81	17	5·2	1·3	0·6	0·8	1·1	1·2	III	209	−67	02−*211*
0235−19	02 35 28	−19 45·2	2·77	15·57	44	13·2	4·2	2·3	0·8	0·9	0·9	III P4·5%	200	−64	02−*110*
0240−42	02 40 41	−42 14·1	2·28	15·29	12	3·7	1·4	1·0	0·8	0·8	0·6		253	−63	02−*410*
0241−51	02 41 52	−51 22·7	1·94	15·22	37	11·8	2·9	0·8	0·7			<10″EW 2nd source or ext to S at 21 and 11 cm	269	−58	02−*53*
0245−55	02 45 27	−55 54·2	1·77	15·01	48	12·2	2·4	1·2	0·9	1·3	1·1	>40″EW	275	−54	02−*54*
0253−23	02 53 58	−23 36·9	2·69	14·51	28	7·8	1·5	0·6	0·8	1·3	1·4	III	212	−62	02−*219*
0319−29	03 19 25	−29 50·5	2·48	12·88		3·8	2·0	1·3		0·5	0·7	III	226	−57	
0319−45	03 19 39	−45 21·8	2·02	12·87	19	9·5	3·4	1·7	0·5	0·8	1·1		254	−55	03−*43*
0320−37	03 20 42	−37 25	2·27	12·84	950	249		89				NGC1316 P10 and 12%	239	−57	03−*31*
0332−39	03 32 17	−39 10·5	2·20	12·01	10	4·5	1·7	0·9	0·5	0·8	1·0		234	−55	03−*32*
0336−35	03 36 48	−35 33·6	2·29	11·71	23	7·9	2·5		0·7	0·9			234	−54	03−*33*

Table 1 (*Continued*)

Catalogue Number	Position (1950)		Annual Precession		Flux Density				Spectrum			Remarks	Galactic Coordinates		MSH Cat. No.
	R.A.	δ	Δα	+Δδ	350	75	21	11	75→350	21→75	11→21	(Ang. Size, Identification, etc.)	l^{II}	b^{II}	
0344−34	03 44 40	−34 31·5	2·30	11·13	33	9·3	3·0	1·7	0·8	0·9	0·9	>45″EW	235	−52	03−*36*
0346−27	03 46 35	−27 59·4	2·47	10·98			1·4	1·3			0·1	III	224	−51	03−*210*
0349−27	03 49 34	−27 53·1	2·47	10·76	53	15·8	5·2	3·1	0·8	0·9	0·8	40″EW >1′NS+fs II	224	−50	03−*212*
												P3·3%			
0354−48	03 54 05	−48 31·8	1·78	10·44	14	3·3	1·2	0·8	0·9	0·8	0·6		257	−49	03−*411*
0357−37	03 57 55	−37 08·9	2·20	10·14	14	3·9	1·6	0·9	0·8	0·7	0·9		239	−49	03−*39*
0411−34	04 11 11	−34 38·0	2·25	9·13	16	4·3	1·5	0·7	0·8	0·9	1·2		235	−46	04−*33*
0411−56	04 11 42	−56 08·5	1·29	9·10	16	4·4	2·5	1·4	0·8	0·5	0·9		266	−44	04−*52*
0413−21	04 13 55	−21 03·0	2·61	8·90	26	6·5	2·5	1·6	0·9	0·7	0·7	III	217	−43	04−*24*
0420−26	04 20 33	−26 22·0	2·46	8·39	11	3·5	1·4	0·7	0·7	0·7	1·1	III	224	−43	04−*26*
0424−26	04 24 41	−26 49·9	2·44	8·29		3·7	1·2	0·6		0·9	1·1	III	225	−43	
0427−36	04 27 52	−36 37·5	2·15	7·82	35	7·2	2·1	1·1	1·0	1·1	1·0		238	−43	04−*36*
0427−53	04 27 51	−53 56·1	1·37	7·82	50	14·6	5·6	2·7	0·8	0·8	1·1	>40″EW 74II P<1·5%	262	−42	04−*54*
0438−43	04 38 42	−43 38·8	1·87	6·93	12	9·3	6·8	6·2	0·2	0·3	0·2	P1%	248	−42	04−*49*
0442−28	04 42 38	−28 14·8	2·40	6·59	82	22	7·1	3·9	0·9	0·9	1·0	35″EW>1·5′+fs <20″NS	228	−39	04−*218*
												III P3·7%			
0443−59	04 43 26	−59 29·7	0·93	6·55		3·6	1·3	0·6		0·8	1·2		269	−39	
0445−22	04 45 36	−22 08·8	2·55	6·35		3·3	2·0	1·0		0·4	1·1	III	221	−36	
0446−20	04 46 25	−20 36·0	2·59	6·28	19	4·2	0·9	0·4	1·0	1·2	1·3	III	219	−36	04−*219*
0451−28	04 51 12	−28 12·4	2·42	5·87		2·7	2·5	2·3		0·1	0·1	II	229	−37	
0453−20	04 53 13	−20 40·5	2·60	5·71	18	9·3	4·7	3·1	0·4	0·5	0·6	I 16mag. EO P1·3%	220	−34	04−*222*
0453−30	04 53 21	−30 11·3	2·33	5·71	43	13·2	3·4	1·9			0·9	III conf.w 0456−30 at	231	−37	04−*314*
												75 cm P4·9%			
0454−22	04 54 05	−22 03·7	2·56	5·65	21	4·3	1·9	1·3	1·0	0·7	0·6	III	222	−35	04−*221*
0454−46	04 54 27	−46 20·5	1·72	5·62	9	4·6	2·6	2·1	0·4	0·5	0·3		252	−39	04−*412*
0455−40	04 55 49	−40 29·9	1·96	5·50	13	3·7	1·0	0·6	0·8	1·0	0·8	ext in RA at 21 cm	244	−38	04−*410*
0456−30	04 56 33	−30 10·8	2·32	5·44			2·7	1·6			0·8	II see 0453−30 P5%	232	−36	

0503−28	05 03 42	−28 59·7	2·34	4·83	30	5·5	1·1	0·6	1·1			II fs<20″NS 2nd source 15′N at 21 cm	231	−35	05−22
0508−22	05 08 53	−22 06·3	2·54	4·34	19	5·1	1·9		0·8	0·8			223	−32	05−23
0511−48	05 11 35	−48 28·0	1·60	4·17	41	13·2	3·5	2·1	0·7	1·3	0·9	≤20″EW	255	−36	05−42
0511−30	05 11 44	−30 31·7	2·30	4·14	29	8·9	2·7	1·2	0·8	1·0	1·3	ext at 11? II>1′NS	233	−33	05−35
0517−56	05 17 36	−56 16·3	1·10	3·66		4·6	1·2	0·8		1·3	0·7		264	−35	
0518−45	05 18 24	−45 49·8	1·72	3·59	570	166	66	30	0·8	0·8		Pictor-A 19mag. galaxy ext at 11 cm P3%	251	−35	05−43
0519−20	05 19 32	−20 50·8	2·57	3·48	19	6·5	2·2	1·0	0·7	0·9	1·2	<20″NS III	223	−28	05−24
0521−36	05 21 14	−36 30·0	2·09	3·34	66	37	18·6	11·4	0·4	0·6	0·7	20″EW P3·5%	240	−33	05−36
0521−32	05 21 42	−32 53·8	2·22	3·29	18	6·7	1·2	0·6			1·1		235	−32	05−37
0523−32	05 23 35	−32 45·1	2·22	3·12			1·2	0·9			0·5		236	−31	
0535−49	05 35 02	−49 45·0	1·51	3·14	16	6·1	2·1	1·0	0·6	1·1	1·1		256	−32	05−46
0541−24	05 41 06	−24 19·4	2·47	1·61	13	2·9	1·1	0·6	1·0	0·8	0·9	III	228	−25	05−27
0546−44	05 46 13	−44 31·3	1·76	1·44	13	4·0	1·5	0·9	0·8	0·8	0·8		251	−30	05−48
0547−40	05 47 48	−40 51·9	1·91	1·03	31	8·5	2·9	1·4	0·8	0·9	1·2	>30″EW	246	−28	05−410
0554−32	05 54 25	−32 23·3	2·22	0·46	14	4·0	1·3	0·8			0·8	2nd source 15′N at 21 cm	238	−25	05−316
0600−34	06 00 36	−34 26·3	2·16	−0·09	22	6·5	1·7		0·8	1·1			240	−24	06−31
0602−31	06 02 24	−31 55·8	2·24	−0·26	17	6·5	2·7	1·9	0·6	0·7	0·6	P<1%	238	−23	06−32
0604−20	06 04 29	−20 22·2	2·58	−0·44	23	8·9	3·3	2·0	0·6	0·8	0·8	III P<2%	227	−19	06−22
0611−25	06 11 32	−25 28·1	2·44	−1·06		2·9	1·1	0·6		0·8	0·9	III	233	−19	
0612−47	06 12 16	−47 26·1	1·61	−1·11	27	5·8	1·2	0·7	1·0	0·8	0·9		255	−26	06−43
0614−34	06 14 49	−34 54·7	2·14	−1·34	7	3·7	2·8	1·9	0·4	0·2	0·6	P1·7%	242	−22	06−36
0616−48	06 16 50	−48 43·9	1·54	−1·51	9	3·1	1·7	1·0	0·7	0·5	0·8		256	−25	06−44
0618−37	06 18 20	−37 10·1	2·06	−1·64	18	6·7	3·0	1·9	0·6	0·7	0·7	P14%	244	−22	06−37
0620−52	06 20 37	−52 39·5	1·32	−1·84	30	9·3	3·4	2·1	0·8	0·8	0·8	P1·3%	261	−26	06−53
0625−53	06 25 18	−53 39·3	1·25	−2·24	113	26	6·7	3·5	1·0	1·1	1·0	20″EW P0·8%	262	−25	06−55
0625−35	06 25 21	−35 26·7	2·12	−2·25	26	9·5	4·5	2·9	0·6	0·6	0·7	P0·5%	243	−20	06−38
0630−27	06 30 29	−27 18·2	2·38	−2·71	12	3·3	1·0	0·5			1·2		236	−16	06−29
0631−27	06 31 40	−27 08·7	2·39	−2·81			0·8	0·5			0·7		236	−16	
0634−20	06 34 25	−20 34·3	2·58	−3·05	67	21	7·0	2·8	0·8	0·9		II fs <20″NS>5′ in δ at 11 cm P6%	230	−12	06−210
0638−27	06 38 07	−27 41·7	2·38	−3·31	17	5·5	1·2		0·7	1·2			237	−15	06−211

TABLE 1 (*Continued*)

Catalogue Number	Position (1950)		Annual Precession		Flux Density				Spectrum			Remarks	Galactic Coordinates		MSH Cat. No.
	R.A.	δ	Δα	+Δδ	350	75	21	11	75→350	21→75	11→21	(Ang. Size, Identification, etc.)	l^{II}	b^{II}	
0642−43	06 42 56	−43 40·6	1·82	−3·77	13	4·3	1·8	1·0	0·7	0·7	0·9		253	−19	06−*412*
0646−39	06 46 33	−39 53·1	1·98	−4·09	26	7·0	2·6	1·5	0·8	0·8	1·0		249	−17	06−*312*
0651−56	06 51 53	−56 38·3	1·08	−4·53	18	4·9	1·1	0·7	0·8	1·2	0·7		266	−22	06−*57*
0656−24	06 56 54	−24 12·5	2·49	−4·98	59	13·0	3·1	1·3	1·0	1·2	1·4	>45″EW 35″NS	235	−9	06−*216*
0700−47	07 00 46	−47 21·2	1·65	−5·28	18	3·4	1·1	0·7	1·1	0·7	0·7		258	−18	07−*41*
0703−45	07 03 57	−45 08·1	1·78	−5·55	25	3·7	0·8	0·4	1·2	1·3		ext in RA at 11 cm	256	−12	07−*42*
0704−42	07 04 22	−42 44·1	1·88	−5·59	19	5·6	1·5	0·8	0·8	1·1	1·0		253	−15	07−*43*
0704−23	07 04 30	−23 07·9	2·52	−5·61	6	7·2	3·8	2·5	−0·1	0·5	0·6	P<1%	236	−6	07−*21*
0707−35	07 07 39	−35 57·0	2·14	−5·87	15	4·6	1·8	0·8	0·8	0·8		ext in RA at 11 cm	247	−12	07−*34*
0709−20	07 09 39	−20 37·3	2·60	−6·02	33	8·7	2·0	1·1	0·8	1·2	1·0		233	−5	07−*23*
0715−25	07 15 16	−25 01·8	2·49	−6·50	17	9·3	4·2	2·8	0·4	0·6	0·6	P4·0%	238	−6	07−*24*
0715−36	07 15 21	−36 15·8	2·13	−6·52	18	7·1	2·2	1·1	0·6	0·9	1·1		248	−11	07−*35*
0718−34	07 18 59	−34 02·5	2·22	−6·79	18	8·6	2·1	1·2			0·9	*S*75 and *S*350 incl. 2nd source	246	−9	07−*37*
0719−55	07 19 13	−55 19·2	1·25	−6·81	24	5·9	2·0	1·2	0·9	0·9	0·8	P<1%	267	−18	07−*53*
0720−52	07 20 08	−52 51·1	1·41	−6·89	13	4·6	1·3	0·7	0·7	1·0	1·0		264	−17	07−*54*
0727−22	07 27 19	−22 12·4	2·57	−7·49	16	6·8	0·8	0·4			1·1	*S*75 and *S*350 incl. 2nd source	237	−2	07−*211*
0727−36	07 27 20	−36 34·3	2·15	−7·49		4·9	2·0	1·3		0·7	0·7		250	−9	
0729−52	07 29 47	−52 30·1	1·45	−7·68	12	3·3	1·1	0·6	0·8	0·9	1·0		264	−15	07−*55*
0735−48	07 35 08	−48 49·1	1·67	−8·11	12	4·9	0·7		0·6			ext at 21 and 11 cm	261	−13	07−*410*
0736−30	07 36 24	−30 19·6	2·36	−8·23	19	4·0	1·4	0·8	1·0	0·9	0·9	III source 2 min. earlier at 21 cm	245	−4	07−*313*
0748−45	07 48 03	−45 28·4	1·88	−9·14	12	4·6	1·8	1·2	0·6	0·7	0·6		260	−10	07−*412*
0748−44	07 48 08	−44 04·7	1·93	−9·14	27	8·0	2·3	1·1	0·8	1·0	1·2		258	−9	07−*413*
0750−26	07 50 27	−26 16·5	2·48	−9·33	13	17·2	11	7·3	−0·2			NGC2467 ext at 21 and 11 cm neb P<1%	243	0	07−*215*

0807−38	08 07 48	−38 56·4	2·16	−10·65	19	8·7	2·3	1·2	0·5	1·1	1·0		256	−3	08−*31*
0814−35	08 14 16	−35 26·3	2·28	−11·12		19·6	5·0	2·5				ext to later RA at 11 and 21 cm P<1%	254	−1	
0819−30	08 19 27	−30 02·8	2·43	−11·49	16	6·5	3·0	1·8	0·5	0·6	0·8	>1′NS	250	+4	08−*23*
0822−52	08 22 30	−52 46·5	1·63	−11·71		5·2	1·7	0·5				ext or multiple source	269	−9	
0825−20	08 25 07	−20 16·3	2·67	−11·90	26	11·7	3·7	2·1	0·5	0·9	0·9		242	+10	08−*24*
0843−33	08 43 10	−33 38·3	2·39	−13·17	17	4·6	2·0	1·3	0·8	0·7	0·7	>1′NS?	256	+6	08−*38*
0847−57	08 47 00	−57 15·1	1·47	−13·35	30	8·9	1·3	0·9			0·6	>30″EW *S*75 and *S*350 incl. 2nd source	275	−9	08−*53*
0850−20	08 50 47	−20 36·0	2·70	−13·65	19	6·2	2·2	1·3	0·7	0·8	0·8		246	+15	08−*216*
0859−25	08 59 37	−25 44·2	2·62	−14·18	54	16·4	5·8	3·3	0·8	0·8	0·9	32″EW P3·2%	252	+13	08−*219*
0902−38	09 02	−38 25	2·32	−14·30	25	12·8	10					∼20′ at 21 cm P1·9%?	262	+5	09−*32*
0903−57	09 03 38	−57 22·1	1·59	−14·41		5·7	2·5	1·8		0·7	0·5		276	−7	
0909−56	09 09 31	−56 23·4	1·73	−14·77		3·7	1·9	1·0		0·5	1·0	RA may be 20s earlier	276	−6	
0916−54	09 16 06	−54 42·7	1·83	−15·16	36	4·9	3·1	1·9			0·8	>30″EW 2nd source 20′N at 21 cm	275	−4	09−*52*
0920−39	09 20 49	−39 46·5	2·36	−15·43	9	3·8	2·4	1·4	0·6	0·4	0·8		265	+7	09−*34*
0935−28	09 35 48	−28 59·1	2·64	−16·23	16	6·0	1·9	1·1	0·6	0·9	0·9	>1′NS	260	+17	09−*27*
0947−24	09 47 38	−24 57·9	2·73	−16·82	9	3·9	1·7	0·9	0·5	0·7	1·0		259	+22	09−*210*
0955−28	09 55 50	−28 50·2	2·70	−17·20	18	6·0	1·4	0·7	0·7	1·2	1·2		263	+20	09−*212*
1002−21	10 02 52	−21 33·3	2·82	−17·51	48	7·7	1·8	0·7	1·2	1·2		<10″EW 30″NS ext at 11 cm	259	+27	10−*21*
1011−31	10 11 33	−31 37·6	2·70	−17·85	10	3·7	1·4	0·9	0·6	0·8	0·7	2nd source 23′S at 21 cm	268	+20	10−*33*
1015−31	10 15 55	−31 28·5	2·72	−18·03	14	5·5	3·5	3·0	0·6	0·4	0·3	P<1·6%	268	+21	10−*35*
1017−42	10 17 39	−42 09·6	2·54	−18·09	51	14·8	1·7	0·8			1·2		275	+12	10−*44*
1018−42	10 18 00	−42 35·9	2·54	−18·11			4·1	2·6			0·7	P2·9%	276	+12	
1030−34	10 30 58	−34 03·4	2·72	−18·56	20	6·2	1·4	0·8	0·8	1·1	0·9		273	+20	10−*38*
1031−40	10 31 13	−40 48·2	2·63	−18·57		4·2	1·2	0·4		1·0		ext at 11 cm	276	+15	10−*410*
1103−24	11 03 47	−24 29·0	2·93	−19·45	8	3·8	1·3	0·7	0·5	0·9	1·0		274	+32	11−*21*
1103−20	11 03 55	−20 52·8	2·95	−19·46	16	5·9	2·4	1·4	0·6	0·7	0·8		272	+35	11−*22*
1107−22	11 07 07	−22 46·5	2·95	−19·52	16	3·5	1·4		1·0	0·7		ext at 11 cm in RA or double	274	+34	11−*23*

TABLE 1 (*Continued*)

Catalogue Number	Position (1950)		Annual Precession		Flux Density				Spectrum			Remarks	Galactic Coordinates		MSH Cat. No.
	R.A.	δ	Δα	+Δδ	350	75	21	11	75→350	21→75	11→21	(Ang. Size, Identification, etc.)	l^{II}	b^{II}	
1116−46	11 16 05	−46 17·9	2·79	−19·68		7·3	2·4	1·6		0·9	0·6		287	+13	
1122−37	11 22 56	−37 06·0	2·91	−19·79	7	4·9	1·3	0·7	0·2	0·8	1·0		284	+22	11−*32*
1123−35	11 23 28	−35 06·7	2·92	−19·79	17	7·2	2·6	1·6	0·5	0·8	0·8		284	+24	11−*33*
1131−19	11 31 02	−19 38·6	3·02	−19·90	32	5·7	1·4	0·8	1·1	1·1	0·9		279	+39	11−*16*
1136−32	11 36 48	−32 05·8	2·99	−19·94	28	5·8	2·5	1·2	1·0	0·7	1·1		285	+28	11−*38*
1138−26	11 38 02	−26 12·9	3·00	−19·96	28	4·1	0·9	0·4	1·2	1·2	1·3		284	+34	11−*27*
1139−28	11 39 04	−28 33·7	3·01	−19·96	27	8·0	2·8	1·5	0·8	0·9	1·0		285	+32	11−*28*
1143−48	11 43 04	−48 19·3	2·98	−19·99	28	9·3	3·3	1·8	0·7	0·8	0·9		292	+13	11−*46*
1143−31	11 43 46	−31 41·2	3·01	−19·99	27	6·2	2·0	0·9	0·9	0·9	1·3		287	+29	11−*310*
1551−34	11 51 51	−34 48·2	3·04	−20·03	10	9·3	6·4	4·2	0·1	0·3	0·7	P2·4%	290	+27	11−*314*
1203−26	12 03 04	−26 17·6	3·08	−20·04		3·7	1·9	1·1		0·5	0·9		290	+35	
1209−52	12 09 28	−52 24·2	3·15	−20·02	182	29	4·6					ext at 11 cm } probably one complex	297	+10	12−*51*
1209−51	12 09 40	−51 57·8	3·15	−20·02			2·6					ext at 11 cm } object	297	+10	
1211−41	12 11 39	−41 43·2	3·13	−20·01	18	5·1	1·6	1·0	0·8	0·9	0·7		296	+21	12−*41*
1215−45	12 15 28	−45 45·2	3·16	−19·99	19	10	5·4	3·2	0·4	0·5	0·8	P<1%	297	+17	12−*43*
1218−53	12 18 36	−53 33·4	3·23	−19·97		5·2	1·3	0·6		1·1	1·2		289	+9	
1221−42	12 21 02	−42 18·7	3·18	−19·95		4·7	2·7	1·6		0·5	0·8		298	+20	
1226−21	12 26 10	−21 09·4	3·12	−19·90	12	3·9	1·3	0·9	0·7	0·9	0·6		296	+41	12−*26*
1233−24	12 33 01	−24 56·0	3·16	−19·83	28	6·4	2·3	1·4	0·9	0·8	0·9		299	+38	12−*27*
1232−41	12 32 59	−41 36·5	3·24	−19·83	11	7·1	2·2	1·0	0·3	1·0	1·3		300	+21	12−*44*
1240−20	12 40 36	−20 55·6	3·17	−19·72		3·0	1·8	1·5		0·4	0·3		300	+42	
1243−53	12 43 10	−53 34·2	3·41	−19·67	17	9·0	1·3	0·7			1·0	*S*75 and *S*350 incl. 1245−53	302	+9	12−*54*
1245−19	12 45 47	−19 42·9	3·17	−19·63		9·4	5·5	3·7		0·4	0·6	P1%	302	+42	
1245−53	12 45 46	−53 36·0	3·41	−19·63			1·2	0·6			1·1		302	+9	
1245−41	12 45 54	−41 01·7	3·30	−19·63	45	10·3	4·1	2·4	1·0	0·8	0·9	<15″EW NGC4696 12·2mag. Sc.P<1%	302	+22	12−*45*

1247−40	12 47 24	−40 09·6	3·20	−19·60		6·4	1·5	0·7		1·2	1·2		303	+23	
1254−30	12 54 40	−30 05·5	3·25	−19·47	28	4·0	1·3		1·2	0·9			304	+33	12−*38*
1257−22	12 57 59	−22 59·8	3·22	−19·39	27	5·3	1·3	0·3	1·1	1·1		ext at 11 cm	306	+40	12−*214*
1259−44	12 59 38	−44 30·4	3·41	−19·35		4·2	1·7	0·9		0·7	1·0		305	+18	
1302−49	13 02 32	−49 12·1	3·50	−19·29	20	14	7·4	4·4	0·2	0·5	0·8	NGC4945 9·2mag.Sc P<1%	305	+13	13−*41*
1309−22	13 09 00	−22 00·9	3·24	−19·12	61	22	5·4	2·6	0·7	1·1	1·1	∼15″EW P<1%	309	+40	13−*23*
1322−42	13 22 24	−42 45	3·50	−18·76	8700							NGC5128 6·1mag.SO Pav 6%	309	+19	13−*42*
1327−21	13 27 23	−21 26·5	3·27	−18·58		5·4	2·0	1·3		0·8	0·7		315	+40	
1328−25	13 28 36	−25 43·8	3·31	−18·51		6·4	1·5	0·9			0·8	*S*75 includes 1329−25	314	+36	
1329−25	13 29 56	−25 43·9	3·31	−18·49			1·3	1·0			0·4	{ IC4296 11·9mag.E	315	+36	
1332−33	13 32 58	−33 37·9	3·41	−18·38	70	32	7·0	3·2				P4% { Also includes	313	+28	13−*33*
1333−33	13 33 44	−33 43·0	3·41	−18·37				1·4				P11% { 1334−33	313	+28	
1334−29	13 34 11	−29 36·3	3·38	−18·36	36	8·5	2·6	1·3	0·9	1·0	1·1	NGC5236 8·0mag.Sc P<4%	315	+32	13−*25*
1334−33	13 34 47	−33 54·2	3·41	−18·36				2·3				P20% ext at 11 cm	313	+28	
1346−39	13 46 53	−39 07·4	3·58	−17·87	22	8·8	2·2	1·1	0·6	1·1	1·1		315	+22	13−*34*
1355−41	13 55 56	−41 38·0	3·63	−17·50	35	13·2	4·6	2·6	0·7	0·8	0·9	P4%	316	+19	13−*45*
1359−35	13 59 39	−35 49·9	3·56	−17·35	20	4·1	1·5		1·0	0·8			319	+24	14−*31*
1400−33	14 00 58	−33 48·0	3·52	−17·28	57	10·3	0·8	0·3	1·1			45″EW ext at 21 and 11 cm NGC5419 12·4mag.EO	320	+27	14−*32*
1411−30	14 11 44	−30 12·4	3·50	−16·78		4·2	1·4	0·7		0·8	1·1		323	+29	
1413−36	14 13 34	−36 27·8	3·60	−16·70		4·4	2·4	1·4		0·5	0·8		321	+23	
1414−21	14 14 32	−21 12·9	3·36	−16·65	17	5·3	1·2	0·6	0·8	1·2	1·1		328	+37	14−*26*
1416−49	14 16 46	−49 22·8	3·97	−16·53	16	6·7	2·6	1·3	0·6	0·8	1·1		317	+11	14−*44*
1420−27	14 20 06	−27 14·2	3·46	−16·37	40	8·9	2·6	1·3	1·0	1·0	1·1	<12″EW	327	+31	14−*28*
1421−38	14 21 14	−38 14·4	3·67	−16·31	20	6·0	2·4	1·2	0·8	0·8	1·1		322	+21	14−*34*
1422−29	14 22 34	−29 47·4	3·53	−16·24	26	7·4	2·5	1·3	0·8	0·9	1·0		326	+29	14−*210*
1424−41	14 24 46	−41 52·9	3·76	−16·13		7·4	3·5	2·5		0·6	0·5	P2·5%	321	+18	
1427−50	14 27 05	−50 30·5	4·03	−15·96	15	5·9	1·5	0·6	0·6	1·1	1·4		319	+9	14−*56*
1445−46	14 45 10	−46 49·6	4·02	−15·01	33	8·7	2·1	1·1	0·8	1·1	1·1		323	+11	14−*49*

TABLE 1 (*Continued*)

Catalogue Number	Position (1950)		Annual Precession		Flux Density				Spectrum			Remarks	Galactic Coordinates		MSH Cat. No.
	R.A.	δ	Δα	+Δδ	350	75	21	11	75→350	21→75	11→21	(Ang. Size, Identification, etc.)	l^{II}	b^{II}	
1451−36	14 51 21	−36 28·8	3·72	−14·65	41	11·5	2·9	1·5	0·8	1·1	1·0		329	+20	14−*38*
1459−41	14 59 11	−41 54·3	3·92	−14·15	55	17·4	4·7	1·4	0·7	1·0		ext in δ at 11 cm	328	+15	14−*415*
1514−24	15 14 47	−24 10·3	3·52	−13·19		5·3	2·7	2·1		0·5	0·4		341	+28	
1518−29	15 18 47	−29 30·8	3·67	−12·91		3·6	1·1	0·6		1·0	1·0		338	+23	
1528−29	15 28 52	−29 18·8	3·68	−12·23		4·1	1·8	0·9		0·7	1·1		340	+22	
1556−21	15 56 08	−21 32·2	3·50	−10·26	36	8·5	2·5	0·8	0·9	1·0		>30″EW ext in δ at 11 cm	350	+23	15−*213*
1602−28	16 02 07	−28 50·4	3·70	−9·80	35	7·6	2·6	1·3	1·0	0·9	1·1		346	+17	16−*21*
1622−31	16 22 41	−31 02·5	3·80	−8·23		4·5	1·6			0·8			348	+13	
1622−29	16 22 56	−29 45·0	3·77	−8·23		6·8	2·2			0·9			349	+16	
1623−22	16 23 19	−22 48·8	3·57	−8·14		4·4	1·5	0·8		0·9	1·0		354	+18	
1643−22	16 43 03	−22 22·1	3·59	−6·56	22	7·6	2·3	1·1	0·7	1·0	1·2		358	+15	16−*29*
1733−56	17 33 20	−56 31·7	5·09	−2·22		20	8·4	4·0		0·7	1·1	P1·3%	335	−13	
1754−59	17 54 35	−59 46·3	5·38	−0·43	25	15	3·9	1·5	0·4	1·1	1·5	P3·2%	334	−17	17−*51*
1814−51	18 14 06	−51 59·1	4·78	1·33	27	14·4	4·2	1·6	0·4	1·0	1·5	<15″EW P2·6%?	343	−16	18−*52*
1821−58	18 21 18	−58 17·7	5·22	1·96		7·6	1·4	0·7			1·1	2nd source sf at 21 cm	336	−20	
1827−36	18 27 37	−36 04·8	4·03	2·49		23	7·4	3·2		0·9	1·3		358	−12	
1830−39	18 30 27	−39 42·2	4·16	2·74		5·4	1·4	0·7		1·1	1·1		355	−14	
1834−43	18 34 04	−43 38·0	4·33	3·05		4·3	2·1	0·9		0·6	1·4		352	−16	
1839−48	18 39 27	−48 39·0	4·57	3·52	41	12	3·7	2·0	0·8	0·9	1·0	>30″EW	347	−19	18−*43*
1840−40	18 40 58	−40 24·7	4·19	3·65	22	7·2	2·9	1·6	0·7	0·7	0·9		356	−16	18−*44*

1910−55	19 10 15	−55 11·4	4·89	5·60		4·0	1·1	0·6		1·0	1·0	74III	342	−25	
1914−45	19 14 04	−45 36·5	4·23	6·44	13	3·5	0·8	0·4	0·8	1·2	1·2	74III	352	−23	19−42
1917−54	19 17 47	−54 38·8	4·86	6·77	27	4·7	0·9	0·3	1·1	1·3		ext at 11 cm?	343	−26	19−52
1928−34	19 28 25	−34 01·7	3·91	7·67		3·1	1·2	0·4		0·8	1·7		5	−22	
1932−46	19 32 20	−46 28·2	4·32	7·91	141	39	13·4	6·9	0·8	0·8	0·9	<10″NS 18″EW P1·2%	353	−27	19−46
1933−58	19 33 18	−58 45·9	5·11	7·99	17	6·8	3·5	1·8	0·6	0·6	1·0		339	−29	19−56
1934−63	19 34 45	−63 49·3	5·49	8·07		6·5	16·6	11·4				Peculiar spectrum P<1%	333	−29	
1940−40	19 40 24	−40 37·8	4·09	8·55	38	5·5	1·6	0·4	1·2	1·0	2·1	>1′NS 30″EW ext in RA at 11 cm?	359	−26	19−410
1946−23	19 46 21	−23 34·6	3·59	9·02		3·4	1·5	0·9		0·7	0·8	III	17	−23	
1951−50	19 51 25	−50 09·9	4·48	9·41	14	4·0	1·5	0·9	0·8	0·8	0·8		349	−30	19−412
1953−42	19 53 40	−42 30·9	4·17	9·56	31	9·7	3·6	1·9	0·7	0·8	1·0	P<1%	357	−29	19−413
1954−55	19 54 21	−55 17·8	4·74	9·64	54	14·8	7·0	4·0	0·8	0·6	0·9	74II>1′NS >40″EW P<1·5%	343	−31	19−57
1955−35	19 55 43	−35 43·3	3·90	9·71	45	9·6	2·4	1·2	1·0	1·1	1·1	74III ∼30″NS ∼20″EW	5	−28	19−35
2002−50	20 02 56	−50 21·6	4·43	10·32		4·4	1·7	0·9		0·8	1·0		349	−32	
2006−56	20 06 31	−56 37·8	4·79	10·55	81	12·2	1·9	0·4	1·2			>35″EW >1′NS 74III ext at 21 cm	342	−33	20−52
2009−52	20 09 33	−52 28·0	4·54	10·77	14	5·2	1·8	1·1	0·6	0·8	0·8		346	−33	20−53
2010−27	20 10 40	−27 34·0	3·66	10·84		2·4	0·9	0·4		0·8	1·3	III	15	−29	
2014−55	20 14 08	−55 49·3	4·71	11·14	19	4·7	1·8	0·7	0·9	0·8		>1′NS 74I ext in δ at 11 cm	343	−34	20−54
2020−57	20 20 28	−57 33·9	4·50	11·57	36	9·2	3·7	1·9	0·9	0·7	1·0	<15″EW 74III	340	−35	20−55
2030−23	20 30 18	−23 02·8	3·52	12·30	22	8·2	3·0	1·6	0·6	0·8	1·0	III	22	−32	20−28
2032−35	20 32 35	−35 05·1	3·81	12·41	41	12·8	6·4	3·7	0·7	0·6	0·8	<10″EW P8%	8	−35	20−37
2039−29	20 39 40	−29 07·3	3·61	12·88		3·5	1·3	0·7		0·8	1·0	III	16	−36	
2040−26	20 40 43	−26 43·8	3·58	12·95	18	6·1	2·3	1·3	0·7	0·8	0·9	>1′NS I 16mag.E	19	−35	20−212
2041−60	20 41 20	−60 30·8	4·87	13·01	55	10·6	2·9	0·9	1·1	1·0	1·8	<15″EW 74I 16mag.galaxy	337	−37	20−61
2048−57	20 48 07	−57 16·4	4·60	13·48	12	6·2	2·1	0·9	0·4	0·9	1·3	IC5063 13mag.SO	340	−39	20−57
2049−36	20 49 08	−36 51·8	3·78	13·54	19	4·3	1·4	0·6	1·0	1·1	1·3		6	−39	20−38
2052−47	20 52 51	−47 26·8	4·13	13·80		3·5	3·0	2·2		0·1	0·5		352	−40	
2053−20	20 53 14	−20 08·2	3·42	13·80	25	6·2	2·8	1·8	0·9	0·7	0·7	II	27	−36	20−214
2058−28	20 58 38	−28 13·3	3·57	14·11	59	15·9	6·7	3·1	0·8	0·7	1·2	⩽20″EW >80″NS I 17mag.E	18	−39	20−215

TABLE 1 (*Continued*)

Catalogue Number	Position (1950)		Annual Precession		Flux Density				Spectrum			Remarks	Galactic Coordinates		MSH Cat. No.
	R.A.	δ	Δα	+Δδ	350	75	21	11	75→ 350	21→ 75	11→ 21	(Ang. Size, Identification, etc.)	l^{II}	b^{II}	
2101—49	21 01 41	—49 01·5	4·14	14·30			1·1	0·7			0·7		350	—42	
2104—25	21 04 23	—25 39·0	3·63	14·48	100	31	12	7·3	0·8	0·8	0·8	>50″EW >1′+fs <20″NS I 16mag.E P<1%	21	—40	21—*21*
2105—48	21 05 24	—48 59·1	4·14	14·54		3·1	1·2	1·0		0·8	0·3		350	—42	
2107—34	21 07 44	—34 03·6	3·83	14·66	14	3·8	1·3	0·7	0·8	0·9	1·0		10	—43	21—*32*
2111—25	21 11 42	—25 53·8	3·62	14·89		3·8	2·6	1·4		0·3	1·0	III	22	—42	
2113—21	21 13 41	—21 08·0	3·50	15·01	24	7·7	2·4	1·4	0·7	0·9	0·9	III	28	—41	21—*23*
2115—30	21 15 08	—30 32·3	3·71	15·12	15	5·7	2·4	1·5	0·6	0·7	0·7		16	—43	21—*34*
2128—20	21 28 13	—20 50·0	3·38	15·79	16	4·6	2·2	1·1	0·8	0·6	1·1	III	30	—44	21—*29*
2130—53	21 30 46	—53 50·3	4·18	16·00	20	5·2	1·6	0·8	0·9	0·9	1·1	74III	342	—45	21—*54*
2140—43	21 40 23	—43 27·1	3·80	16·46	27	10	3·7	1·7	0·6	0·8	1·2	>40″EW P4%	357	—49	21—*47*
2149—28	21 49 12	—28 43·0	3·46	16·86	12	5·4	3·2	1·9	0·5	0·4	0·8	III	20	—50	21—*214*
2150—52	21 50 50	—52 04·6	3·99	16·95	28	10	4·2	2·1	0·7	0·7	1·1	74III 30″EW P1%	344	—49	21—*58*
2201—55	22 01 44	—55 32·8	3·86	17·44		4·9	2·1	1·0		0·7	1·2		338	—49	
2204—54	22 04 26	—54 01·4	3·89	17·57		3·2	2·4	1·8		0·2	0·4	74II	340	—50	
2207—45	22 07 15	—45 57·7	3·82	17·69		5·9	1·6	0·9		1·0	0·9		352	—53	
2207—43	22 07 57	—43 48·4	3·63	17·69	13	4·0	1·1	0·7	0·8	1·0	0·7		355	—54	22—*42*
2210—25	22 10 12	—25 43·3	3·36	17·81		3·2	1·3	0·9		0·7	0·6	III	27	—54	
2213—45	22 13 49	—45 36·4	3·68	17·93		5·6	2·3	1·3		0·7	0·9		352	—54	
2216—28	22 16 56	—28 12·1	3·37	18·09		6·8	2·6	1·0		0·8	1·5		22	—56	

2218—50	22 18 05	—50 33·8	3·76	18·16	16	6·3	2·0	0·8			1·4		345	—54	22—*51*
2220—50	22 20 26	—50 32·6	3·76	18·22			1·2	0·7			0·9		344	—54	
2223—52	22 23 50	—52 49·4	3·78	18·35	30	7·9	3·0	1·4	0·9	0·8	1·2	∼15″EW	340	—53	22—*52*
2226—41	22 26 25	—41 07·3	3·53	18·42	28	8·9	3·2	1·6	0·7	0·8	1·1		359	—58	22—*43*
2226—38	22 26 52	—38 39·7	3·49	18·42		8·4	2·6	0·9		1·0	1·7		3	—58	
2244—37	22 44 15	—37 14·2	3·38	18·98		3·9	1·8	0·9		0·6	1·1		4	—62	
2250—41	22 50 07	—41 14·3	3·70	19·11	42	12·8	5·2	2·5	0·7	0·7	1·1	30″EW P2·1%	355	—62	22—*46*
2252—53	22 52 48	—53 01·4	3·62	19·18	22	7·0	3·5	1·7	0·7	0·6	1·1		335	—56	22—*54*
2253—52	22 53 48	—52 14·9	3·56	19·21	28	7·8	3·1	1·3	0·8	0·8	1·3	⩽15″EW	336	—57	22—*55*
2259—37	22 59 37	—37 34·2	3·23	19·36	21	6·8	3·1	1·7	0·7	0·6	0·9		3	—65	22—*35*
2305—41	23 05 06	—41 49·3	3·36	19·47		4·4	1·9	0·9		0·7	1·2		352	—64	
2310—41	23 10 07	—41 43·0	3·23	19·58		4·4	1·8	0·9		0·7	1·1		352	—65	
2317—27	23 17 19	—27 44·5	3·19	19·69	23	9·2	3·3	1·8	0·7	0·8	0·9	>1′NS	28	—69	23—*24*
2319—55	23 19 14	—55 02·5	3·40	19·72		4·5	2·2	1·0		0·6	1·3	74III	327	—58	
2323—40	23 23 51	—40 44·3	3·25	19·79	15	8·0	3·9	2·2	0·5	0·6	0·9		352	—68	23—*43*
2331—41	23 31 45	—41 42·8	3·21	19·89	50	15·6	5·7	2·9	0·9	0·8	1·1	26″EW ∼30″NS P0·7%	346	—69	23—*44*
2334—35	23 34 14	—35 01·8	3·17	19·91	24	4·5	1·3	0·6	1·1	1·0	1·2		3	—72	23—*34*
2338—58	23 38 31	—58 32·4	3·26	19·96	25	7·4	3·3	1·8	0·6	0·6	0·7	74III	320	—57	23—*52*
2354—35	23 54 27	—35 02·4	3·09	20·04	39	5·9	1·3	0·5	1·2	1·2	1·6	>40″EW	356	—76	23—*37*
2356—61	23 56 24	—61 11·7	3·09	20·04	296	66	21	11	1·0	1·0	1·0	40″EW 74II P4·9%	314	—55	23—*64*

Errors in the altazimuth system (Δz-altitude and Δx-azimuth) arise from the following causes:

(1) Misalignment between the electrical phase centre and the mechanical centre of the feed (affects both Δz and Δx).

(2) Misalignment between the mechanical centre of the feed and the intersection of the axis of the reflector and the focal plane (affects both Δz and Δx).

(3) Misalignment between the axis of the error detector and the axis of the reflector (affects both Δz and Δx).

(4) Deflection of the reflector and the feed support structure with changing zenith angle (affects Δz only).

(5) Refraction, which, with an altazimuth mount, we can choose to consider a telescope error (affects Δz only).

The various components are not easy to determine separately and for correction purposes it is only necessary to know the effect of the sum. However, it is in practice desirable to reduce each to the minimum possible. (1) can be determined by measuring the apparent position of a source at different feed angles and (2) by direct survey techniques. At the zenith (3) can be determined from the variation in outputs of the error detector as the main telescope is rotated with both it and the master unit pointing near the zenith.

The resultant errors in right ascension and declination may be written

$$\Delta\alpha \text{ (in seconds of time)} = 4 \sec \delta \, (\Delta x \cos q + \Delta z \sin q),$$

$$\Delta\delta \text{ (in minutes of arc)} = -\Delta x \sin q + \Delta z \cos q,$$

where $\Delta z = f(z)$ and Δx are in minutes of arc and q is the parallactic angle (positive before transit). Δx and Δz for $z \approx 0$ can be determined from observations near transit of a source which passes close to the zenith but whose position is not necessarily accurately known. Near transit q changes from $+90°$ to $-90°$ while the zenith angle hardly varies. Δz as a function of z can be determined from observations of the same source or by observation of the apparent declinations of calibrator sources near transit. These observations, of course, must be corrected for the known master equatorial errors.

In practice errors (1) and (2) have been reduced to negligible proportions. The sum of the zenith angle components of (3), (4), and (5) now changes from 0 to $1 \cdot 7'$ between zenith angles 0° and 60° and compensation is injected into the error detection system to allow for it. Compensation will also be introduced to allow for the azimuth component, which varies from 0 to $0 \cdot 4'$ with changing zenith angle.

There are two other small sources of error intermediate between the two systems. One is due to a small lag in the servo system. The amplitude of this error is directly indicated on the control desk and, except in the case of high wind gusts, does not exceed a few seconds of arc. The second is due to variation in the collimation between the axis of the optical telescope in the master unit used in its calibration and the normal to the reflecting plane mirror. Its amplitude is of the order of 5″ of arc between +4 and —4 hr hour angle; however, it exhibits some hysteresis and at present no systematic corrections are applied to compensate for it.

Very few of the survey positions have been measured with the instrument in its present state and corrections of as much as 1·5′ have been applied to the various sets of observations from correction tables provided by Roberts. Telescope adjustments based on deductions from the correction tables have generally resulted in a reduction of errors of the order expected. Nevertheless, errors of as much as 0·3′ for sources with declinations north of —40° and perhaps twice as much near —60° could be due to an inadequate knowledge of the corrections.

In view of the magnitude of these errors we did not apply second-order precession corrections, giving a further small source of error.

A comparison between corrected positions obtained at 21 and 11 cm at different times showed median differences of 0·45′ in both coordinates. These differences would include differential errors in the correction tables, differences in second-order precession, and effects due to both signal and confusion noise. The latter effects do not appear to be serious, as the median differences between the 21 and 11 cm positions are almost independent of source intensity, being about 0·40′ for the 100 most intense and 0·45′ for the total 300.

Taking into account all the sources of error discussed, we believe that the errors in the catalogue positions do not exceed 0·6′ for 90% of the sources over most of the zone. Between declinations —50° and —60° the uncertainty may increase to $\sim$1·0′.

VIII. Notes on the Catalogue

Table 1 lists the details of the 297 sources in the declination zone —20° to —60°. The table is largely self explanatory. Details of the individual columns are as follows:

Column 1.—Catalogue number consisting of the hours and minutes of right ascension and the sign and degrees of declination. This has one more digit than in the MSH or IAU system but has the advantages that it specifies position quite closely and permits interpolation of additional sources with no basic change in the numbering system.

Columns 2 and 3.—The position for epoch 1950. For a discussion of errors see Section VII.

Columns 4 and 5.—The annual precession in right ascension and declination. The sign of the declination correction is indicated at the top of column 5.

Columns 6, 7, 8, and 9.—Flux densities in units of 10^{-26} W $m^{-2}(c/s)^{-1}$ at wavelengths of 350, 75, 21, and 11 cm. The value at 350 cm is taken from MSH; where a source is a blend at the longer wavelengths and resolved at the short wavelengths this fact is indicated by placing the 75- and 350-cm flux densities midway between adjacent rows, or by a note in column 13. In the case of "extended" sources where two values of flux density are quoted in MSH the smaller or "peak" value is used if the source is not resolved at the short wavelengths. Peak rather than integrated values for extended sources are also given at 21 and 11 cm except where noted in column 13. For a discussion of the flux density scales and errors see Section VI.

Columns 10, 11, and 12.—The spectral indices* for the ranges 11–21, 21–75, and 75–350 cm. If the flux densities are in doubt owing to possible extension or blending, the spectral indices for the appropriate ranges are omitted.

Column 13.—Miscellaneous data. These data involve the classification of the optical field of the source (Roman numerals—see Section IX), data on angular sizes, polarization, and identifications. Angular sizes denoted EW are taken from MSH and refer to interferometric observations from two east–west base lines. Angular sizes denoted NS are preliminary estimates from interferometric observations at four north–south base lines. These were kindly supplied by Dr. P. A. G. Scheuer in advance of publication. Polarization is indicated by a P followed by a percentage and refers to 21 cm observations only.

Columns 14 and 15.—New galactic coordinates.

Column 16.—MSH catalogue numbers.

Abbreviations used in column 13.—

I, II, III, IV—field class on 48-in. Sky Survey Plate,

74 followed by one of the above—field class on 74-in. Stromlo Plate,

EW—east–west angular size,

NS—north–south angular size,

N—north, S—south,

P—polarization,

S75—flux density at 75 cm etc.

conf. w—confused with,

ext—extended,

f—following,

fs—fine structure,

p—preceding.

IX. Identifications

The positions of all of the 297 sources in the catalogue have been compared with the position of galaxies and emission nebulae in the NGC. One object agrees in position with an emission nebula, NGC 2467, and the agreement between the radio and optical dimensions and the radio spectrum makes the identification certain. Nine of the sources agree in position with galaxies brighter than photographic magnitude 12·5. These include the two well-known identifications NGC 5128 and NGC 1316; the remainder have been previously suggested as identifications by Mills, Slee, and Hill.

The positions of 68 sources have been examined on prints of the Palomar Sky Survey or on plates taken with the 74-in. Mount Stromlo reflector. We are indebted to Professor Bart J. Bok and the staff of Mount Stromlo Observatory, in particular Dr. Bengt Westerlund, for taking these plates and also to Miss Lindsey Smith for measuring positions on them. The source fields have been classified in the system first used by Harris and Roberts (1960).

* Previously the spectral index has been derived from $S = f^x$, where x is the spectral index. We have adopted the *opposite sign* throughout this paper to avoid the continuous use of a minus sign.

Class I: The error rectangle about the source position includes a galaxy brighter than $m_{pg} = 17$.

Class II: The area includes a galaxy or galaxies brighter than $m_{pg} = 19 \cdot 5$ and fainter than $m_{pg} = 17$.

Class III: The area includes no galaxies above plate limit.

Class IV: The field is heavily obscured.

A field of Class I is not necessarily equivalent to a certain identification. In the case of source positions in clusters of galaxies the error rectangle may include faint galaxies as well as an outstanding bright object. The distribution of the 68 sources between the various classifications is: I, 9; II, 15; III, 44. If we include the fraction of NGC objects given by the ratio of the number of sources for which plates were examined to the total this would revise the figures to I, 11(16%); II, 15(21%); and III, 44(63%). As has been found in previous such investigations, a large fraction of the sources are optically faint and presumably very distant objects.

Identifications considered definite are listed in Table 2 and identifications considered probable are listed in Table 3. The magnitudes and types of the identified galaxies, particularly from the Mount Stromlo plates, should be considered as preliminary; no attempt was made to standardize the plates, which were taken under variable weather conditions and at a variety of exposures.

X. Source Counts

This survey gives the flux densities of some 300 sources at three different wavelengths; for 80% of these, flux densities are available at a further wavelength from MSH. Although both the total number and the number per steradian are slightly lower than for some previous surveys, for example MSH, we believe the data are better suited for investigating the well-known number-flux density relation. The basic survey at 75 cm was carried out with a filled-aperture telescope, with a very favourable signal–noise ratio even for the weakest sources, and with the source selection made at a level of one source per 70 beamwidths. Furthermore, the catalogue includes only objects whose existence has been confirmed by observation at two shorter wavelengths with correspondingly higher resolving power.

The relation between the number of sources above a given level of flux density and the flux density is shown in Figure 4. Curves are given for the results at the four wavelengths, all of which give a slope of $-1 \cdot 85$.

At the survey wavelength, the departure from the $-1 \cdot 85$ slope occurs very close to the intended limit of the survey. Dispersion in spectral indices is responsible for the somewhat earlier breakaway at the other three wavelengths. As mentioned in Section III, 12 of the 75-cm sources were resolved into doubles at 21 cm. In the source counts, physical doubles (NGC 1316, NGC 5128, and IC 4296) have been counted as one source and the non-physical doubles as two sources, with the 75-cm flux densities apportioned in the ratio of their 21-cm components. That these other nine objects are non-physical doubles may be argued from the fact that to be

Table 2

CERTAIN IDENTIFICATIONS

Source	Radio Position	Optical Position	Remarks
0045−25 (00−*222*)	$00^h45^m06^s$ −25°33′·4	$00^h45^m\cdot1$ (Becvar) −25°34′	NGC 253 7·0 mag. Sc
0131−36 (01−*311*)	$01^h31^m42^s$ −36°44′·6	$01^h31^m43^s\cdot7$ −36°44′56″	15 mag. SO
NGC 1316 (Fornax–A)	$03^h20^m42^s$ −37°25′	$03^h20^m\cdot7$ (Becvar) −37°25′	10·1 mag. SO
Pictor–A	$05^h18^m24^s$ −45°49′·8	$05^h18^m24^s\cdot1$ (Minkowski) −45°49′·8	19 mag. galaxy
0750−26 (07−*215*)	$07^h50^m27^s$ −26°16′·5	$07^h51^m\cdot3$ (Becvar) −26°16′	NGC 2467, emission nebula
1245−41 (12−*45*)	$12^h45^m54^s$ −41°01′·7	$12^h46^m\cdot1$ (Becvar) −41°02′	NGC 4696 12·2 mag. SO
1302−49 (13−*41*)	$13^h02^m32^s$ −49°12′·1	$13^h02^m\cdot4$ (Becvar) −49°01′	NGC 4945 9·2 mag. Sc
NGC 5128 (Centaurus–A)	$13^h22^m24^s$ −42°45′	$13^h22^m28^s$ (Baade and Minkowski) −42°45′·6	6·1 mag. SO
1333−33 (13−*33*)	$13^h33^m44^s$ −33°43′·0	$13^h33^m\cdot8$ (Becvar) −33°43′	IC 4296 11·9 mag. E
1334−29 (13−*25*)	$13^h34^m11^s$ −29°36′·3	$13^h34^m\cdot3$ (Becvar) −29°37′	NGC 5236 8·0 mag. Sc
2014−55 (20−*54*)	$20^h14^m08^s$ −55°49′·3	$20^h14^m06^s\cdot1$ (Westerlund) −55°48′51″	16 mag. E
2048−57 (20−*57*)	$20^h48^m07^s$ −57°16′·4	$20^h48^m\cdot2$ (Becvar) −57°16′	IC 5063 13 mag. SO

resolved at 21 cm (i.e. have a component separation of $\geqslant 15'$) the source should be easily identifiable; alternatively, from knowledge of the nature of physical doubles the individual components should themselves appear extended at 11 cm.

TABLE 3

PROBABLE IDENTIFICATIONS

Source	Radio Position	Optical Position	Remarks
0023−33 (00−38)	$00^h23^m02^s$ $-33°20'\cdot1$	$00^h23^m02^s\cdot2$ (Westerlund) $-33°19'22''$	16 mag. E
0043−42 (00−411)	$00^h43^m52^s$ $-42°24'\cdot3$	$00^h43^m52^s\cdot8$ (Westerlund) $-42°24'13''$	17 mag. galaxy
0114−47 (01−45)	$01^h14^m05^s$ $-47°38'\cdot1$	$01^h14^m14^s\cdot8$ (Westerlund) $-47°38'29''$	17 mag. galaxy
0427−53 (04−54)	$04^h27^m51^s$ $-53°56'\cdot1$	$04^h27^m58^s$ (Westerlund) $-53°51'\cdot1$	close pair 17 mag. galaxies
0453−20 (04−222)	$04^h53^m13^s$ $-20°40'\cdot5$	$04^h53^m13^s$ (Bolton) $-20°39'\cdot3$	16 mag. EO
0634−20 (06−210)	$06^h34^m25^s$ $-20°34'\cdot3$	$06^h34^m22^s$ (Bolton) $-20°32'\cdot4$	17 mag. galaxy
2040−26 (20−212)	$20^h40^m43^s$ $-26°43'\cdot8$	$20^h40^m45^s\cdot6$ (Bolton) $-26°43'\cdot3$	16 mag. E
2041−60 (20−61)	$20^h41^m20^s$ $-60°30'\cdot8$	$20^h41^m12^s\cdot7$ (Westerlund) $-60°30'20''$	16 mag. galaxy
2058−28 (20−215)	$20^h58^m38^s$ $-28°13'\cdot3$	$20^h58^m38^s\cdot2$ (Bolton) $-28°13'\cdot6$	17 mag. E
2104−25 (21−21)	$21^h04^m23^s$ $-25°39'\cdot0$	$21^h04^m25^s$ (Bolton) $-25°39'\cdot5$	16·5 mag. E

The slope of the log N–log S relation of $-1\cdot85$ ($\pm0\cdot1$) is in very good agreement with the value of $-1\cdot80\pm0\cdot1$ to which the Cambridge source counts have converged (Ryle 1963) for the equivalent range of flux densities. It is interesting to note that the 350-cm slope differs appreciably from the $-1\cdot5$ value of Mills, Slee, and Hill (1960) for all the sources in their catalogue. The fact that the 21- and 11-cm slopes also agree with the 75-cm slope suggests that number–flux density relation at one wavelength is unaffected by source selection at another (apart from the breakaway at low flux densities).

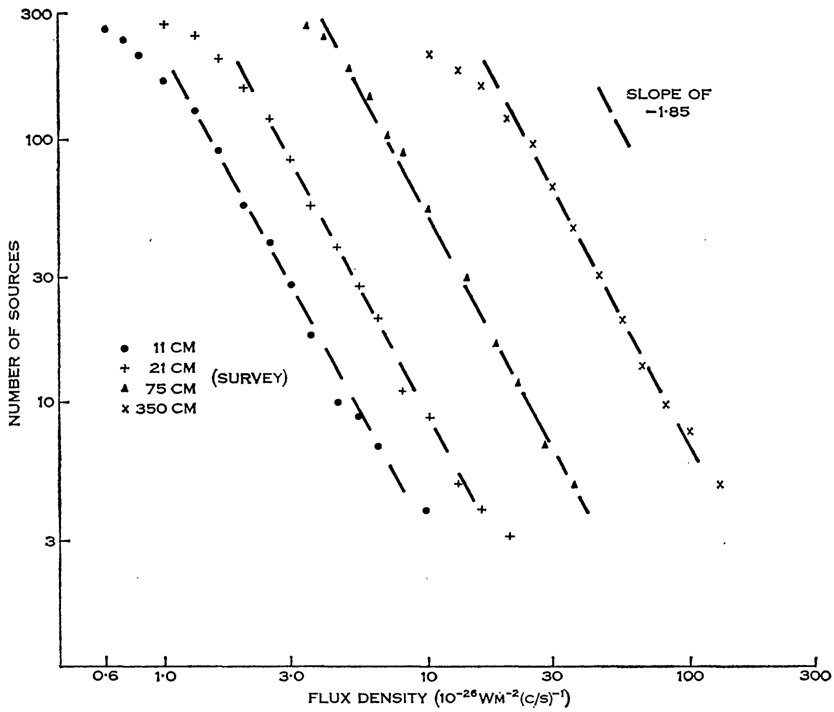

Fig. 4.—Source counts at four wavelengths for the survey area. The ordinate is the number of sources above a certain flux density level and the abscissa is the flux density. The 350-cm (85 Mc/s) data are from Mills, Slee, and Hill, but refer only to the sources in this catalogue.

XI. Spectra of Sources

Columns 10, 11, and 12 of the catalogue table give the spectral indices of the source for the three individual wavelength ranges available: 11–21, 21–75, and 75–350 cm. No indices are given in cases where the data are at all suspect, e.g. where extension of a source or confusion due to neighbouring sources may have affected the flux densities. In view of the possible errors in flux densities already discussed, errors in the indices of $0\cdot1$ would be fairly common but errors greater than $0\cdot3$ very rare. Thus the series of indices $0\cdot8$, $0\cdot6$, $0\cdot7$ could very well indicate a straight-line spectrum but $0\cdot1$, $0\cdot3$, $0\cdot6$ would almost certainly possess a real and large curvature. In most such extreme cases as the last example, repeat observations were made to check the individual flux densities.

The distributions of the spectral indices of the sources in the three wavelength ranges are shown in Figures 5(*a*), 5(*b*), and 5(*c*). Two results can be seen; firstly that the dispersion increases with decreasing wavelength, and secondly that the median spectral index increases with decreasing wavelength from 0·76 at the long wavelength end through 0·83 to 0·96 at the short wavelength end. This trend in median index could, of course, be due to calibration errors but the dispersion

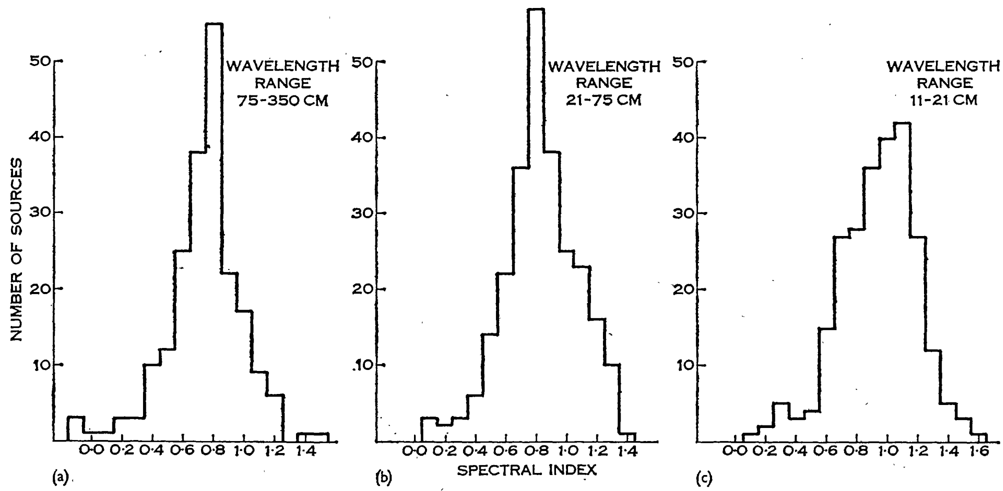

Fig. 5.—Histograms of the distribution of spectral indices in three different wavelength ranges: (*a*) 75–350 cm, (*b*) 21–75 cm, and (*c*) 11–21 cm.

effect could not. As the calibration of scales is connected via the CKL scales to such objects as the Crab nebula and emission nebula, where the forms of the spectra are well known, we believe both effects are genuine. The shift in the median index

Table 4

SOURCES WITH CURVED SPECTRA

Positive curvature sources:			
0045−25	0049−43	0114−21	0122−25
0129−51	0221−28	0319−45	0535−49
0715−36	0807−38	0947−24	1103−24
1122−37	1151−34	1232−41	1302−49
1346−39	1416−49	1427−50	1643−22
1754−59	1814−51	2048−57	
Negative curvature sources:			
0454−22	1015−31		
Reversing curvature sources:			
0126−53	0216−36	0220−42	
Positive curvature with a maximum in the wavelength range:			
0023−26	0704−23	1934−63	

and the change in dispersion is probably influenced by the tendency for the spectra of many individual sources to steepen at short wavelengths (positive curvature). Such curvature has been related to the brightness temperature of the sources by Kellermann *et al.* (1962).

Whereas most spectra approximate to straight power laws, there is a wide variety of form among the remaining small fraction. These sources are listed in Table 4 under four classifications. These classifications are (1) positive curvature where the index increases with decreasing wavelength, (2) negative curvature, (3) reversing curvature, and (4) positive curvature with a maximum flux density within the wavelength range. Examples of these various types are given in Figures 6(*a*)

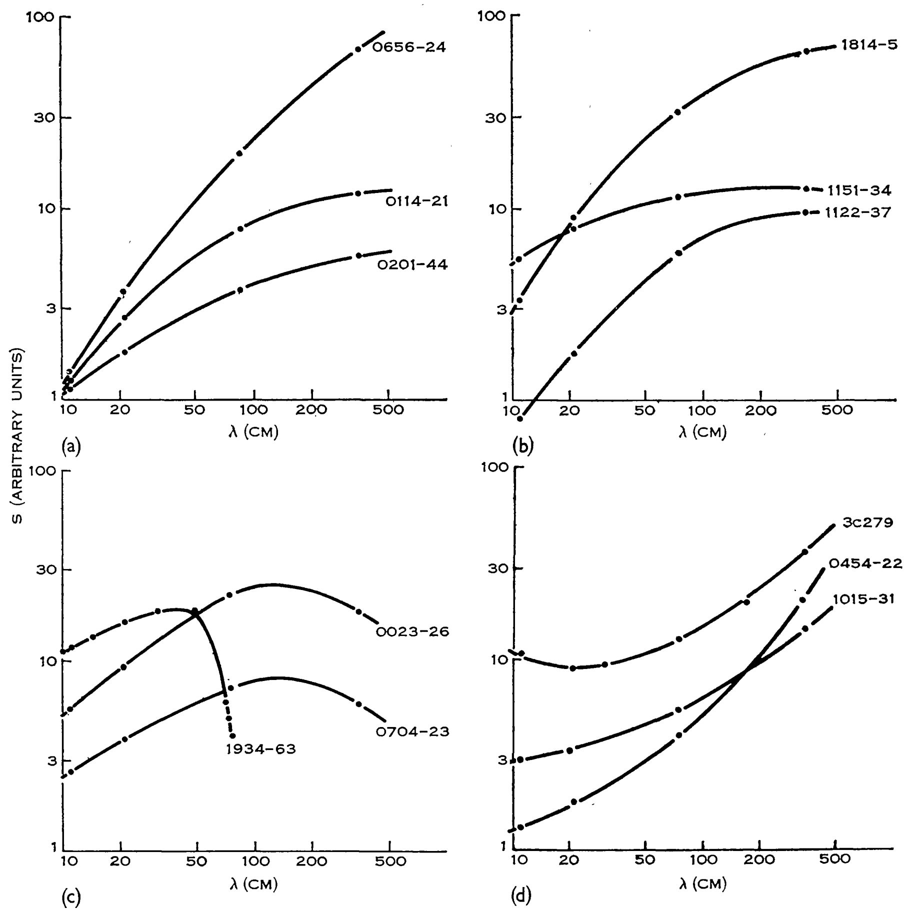

Fig. 6.—Samples of curved spectra: (*a*) and (*b*) positive curvature spectra; (*c*) positive curvature with maxima in the observed wavelength range; and (*d*) negative curvature with and without minima in the wavelength range.

to 6(*d*). 3c 279 has been included in Figure 6(*d*), although it is not in the survey zone. F. T. Haddock (1963) has also reported a number of similar cases at very short wavelengths. The spectra of positive curvature have been explained in terms of synchrotron decay in evolving sources. Objects of negative curvature could be explained as being due to double sources, one of which has a spectrum of type 4 and the other a straight spectrum. Three of the sources of strong positive curvature are identified with relatively nearby Sc galaxies (NGC 253, NGC 4945, IC 5063) where the radiation is believed to be confined to small regions near the nuclei of these systems.

XII. Polarization and Spectra

An interesting statistical relationship has been found between the percentage polarization of a source and both its spectral index and spectral curvature. Table 5 shows the distribution of sources between various classes of polarization and spectral index. Above 5% linear polarization the sources are confined to spectral indices

Table 5

DISTRIBUTION OF SOURCES BETWEEN POLARIZATION AND SPECTRAL INDEX CLASSES

Polarization Percentage	Spectral Index		
	< 0·7	0·7–0·9	> 0·9
> 5	0	9	0
< 5	17	25	5
> 2	4	22	2
< 2	13	12	3

between 0·7 and 0·9. Table 6 gives a similar breakdown of sources into spectral curvature classes where the curvature is defined as the difference between the short wavelength (11–21 cm) and the long wavelength (75–350 cm) indices. Here the highly polarized sources are almost exclusively confined to the low curvature range.

Table 6

DISTRIBUTION OF SOURCES BETWEEN POLARIZATION AND SPECTRAL CURVATURE CLASSES

Polarization Percentage	Spectral Curvature		
	0 or 0·1	0·2–0·5	> 0·5
> 5	9	1	0
< 5	21	17	11
> 2	18	5	6
< 2	12	13	5

Kellermann *et al.* (1962) have shown that sources of high spectral curvature are associated with sources of very high brightness temperature. These are sources of relatively small physical dimensions, perhaps rather young on an evolutionary scale, and they probably have highly turbulent magnetic fields. Gardner and Whiteoak (1963) have suggested that the highly polarized sources at 21-cm wavelength are of low surface brightness. They are perhaps of large physical size and may represent older sources on an evolutionary scale, whose magnetic field may have developed a high degree of order. The new relationships are consistent with both of these hypotheses and may further assist in classification of sources. Combination of polarization and spectral characteristics may provide a clue to the absolute physical size of a source, which, combined with a measure of angular diameter, will give both distance and absolute luminosity. This would be particularly valuable where optical identification could not be made for reasons such as interstellar absorption, and as a guide in making identification in unobscured regions.

XIII. Comparison of the Present Survey and MSH

(*a*) *Comparison of Sources*

Of the 297 sources listed in this catalogue, 51 do not appear in MSH. Two-thirds of these occur in the second half of our catalogue (MSH have commented on a deficiency in this part of their catalogue) and nine of them are between 22^h and 23^h R.A. While a small number can be accounted for in terms of spectra, the majority must be due to instrumental effects in the MSH observations, such as shielding due to strong sources in the side lobes of the cross, interference, etc.

The reverse comparison is more difficult because of the lack of spectral information. The intended limit of the 75-cm survey was 4 f.u. At 5 f.u., judging by the log N–log S curve, the survey is complete with very safe limits. With the median spectral index, a source of 5 f.u. at 75 cm would have a value of 16 f.u. at 350 cm; for a source of 4 f.u. the value would be 13 flux units. For an index of 1·0 (which includes all but 5% of sources in Fig. 5(*a*)) the values corresponding to 4 and 5 f.u. at 75 cm are 19 and 24 f.u. respectively at 350 cm. In the survey area there are 90 sources in MSH of flux density greater than 16 f.u. and 23 greater than 20 f.u. not in the present catalogue.

The areas in the vicinity of a sample of 20 of these sources were investigated at 75 and 21 cm with the following results.

(1) Seven of the sources showed no trace on the 75-cm survey records and no sources were found in an area of one square degree about the MSH position at 21 cm. The sources with their flux densities in brackets, are:

03–2*3*(23)	13–4*4*(32)	14–3*5*(16)
14–4*6*(29)	15–2*3*(20)	16–3*5*(24)
16–3*6*(29)		

For both 16–3*5* and 16–3*6* there are fairly strong sources about 1° away from each position.

(2) Two of the sources were not visible on the survey records. At 21 cm weak sources (< 0·5 f.u.) were found within the 1° area but poor agreement in position suggests they are chance coincidences. These are:

07–2*2*(22)	12–3*4*(22)

(3) Seven of the sources had possible traces on the survey records. Weak sources (< 0·5 f.u.) were found within the 1° area but poor agreement in position suggests they are chance coincidences. These are:

00–5*2*(12)	02–4*7*(14)	06–2*15*(16)
07–2*12*(24)	08–4*1*(27)	12–3*9*(18)
14–4*6*(29)		

(4) Four sources appeared on the 75-cm survey records but below the selection level for the catalogue; at 21 cm they were also detected in positions in good agreement with the MSH positions. These are:

01−5*8*(20) 05−3*18*(16) 05−3*19*(20)
07−4*14*(18)

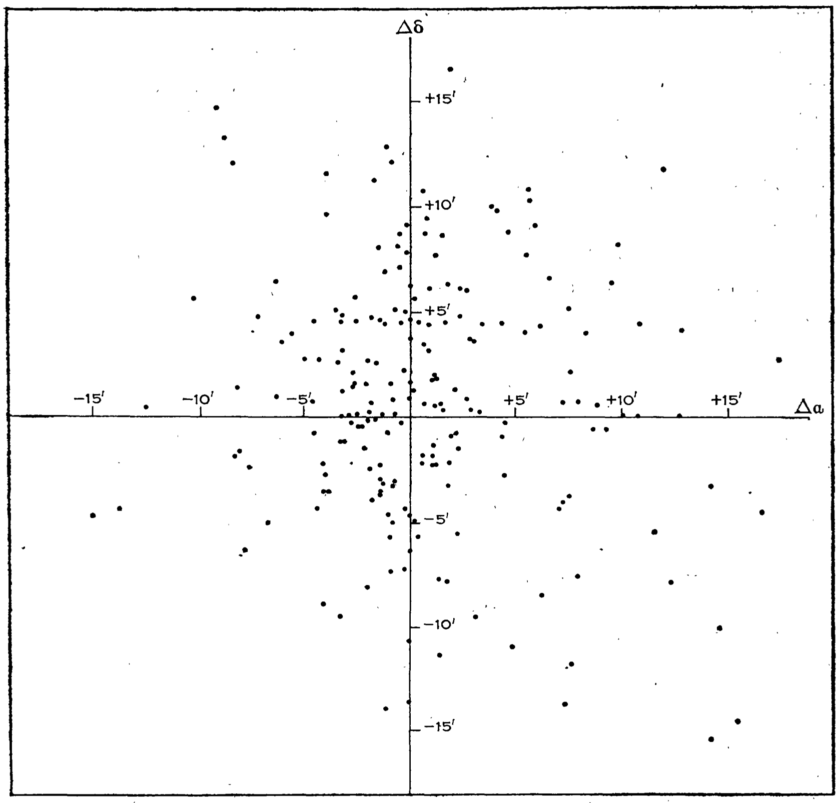

Fig. 7.—The differences between the positions of sources measured at 21 cm and those given by MSH. Eight sources lie outside the limits of this diagram.

These sources appear to have spectral indices of the order of 1·2 in the range from 21 to 350 cm. From this sample investigation we conclude that a limited number of the discrepancies are due to objects of high spectral index but that the great majority cannot be accounted for. Resolution of extended objects might explain failure to detect them at 21 cm but not at 75 cm.

(*b*) *Comparison of Positions*

A comparison of the MSH positions and those of the present catalogue is shown in Figure 7. The median difference is 8′ of arc distributed fairly equally between both coordinates, i.e. 5·6′ in each. The medians of the probable errors given in the MSH catalogue for these sources are 3·5′ of arc in right ascension and 5′ in declination. Thus the MSH estimates of position uncertainty appears to have been fairly accurate.

(c) *MSH Extended Sources*

A separate investigation has already been made with the 210-ft telescope of some of the controversial "extended" and "probably extended" sources in the MSH catalogue by Milne and Scheuer (1964). These authors find a variety of explanations for the origin of these objects. We have not carried out such a detailed investigation but merely noted the characteristics of sources apparently associated with the extended objects in the survey zone.

Of 15 sources listed as "extended", 6 (including NGC 1316 and NGC 5128) were found to be double or extended sources at 21 cm. In the other 9 cases the region contained only one dominant unresolved source. The MSH "peak" flux density is in good agreement with the flux density expected from the shorter wavelength observations, that is, the sources are real but not extended.

Of 18 sources listed as "probably extended", 3 were resolved into doubles at 21 cm and the remainder were unresolved. We note that 5 sources which were not given as extended in MSH were clearly resolved into doubles in our own observations at 21 cm.

XIV. References

Bennett, A. S., and Smith, F. G. (1961).—*Mon. Not. R. Astr. Soc.* **122**: 71.
Bowen, E. G., and Minnett, H. C. (1962).—*J. Brit. Instn. Radio Engrs.* **23**: 49.
Conway, R. G., Kellermann, K. I., and Long, R. J. (1963).—*Mon. Not. R. Astr. Soc.* **125**: 261.
Cooper, B. F. C., Cousins, T. E., and Gruner, L. (1964).—*Proc. Instn. Radio Engrs. Aust.* **25**: 221.
Gardner, F. F., and Milne, D. K. (1963).—*Proc. Instn. Radio Engrs. Aust.* **24**: 127.
Gardner, F. F., and Whiteoak, J. B. (1962).—*Phys. Rev. Letters* **9**: 197.
Gardner, F. F., and Whiteoak, J. B. (1963).—*Nature* **197**: 1162.
Haddock, F. T. (1963).—Report at XIII General Assembly of URSI, Tokyo.
Harris, D. E., and Roberts, J. A. (1960).—*Publ. Astr. Soc. Pacif.* **72**: 427.
Kellermann, K. I., and Harris, D. E. (1960).—Obs. Caltech Radio Observatory No. 7.
Kellermann, K. I., Long, R. J., Allen, L. R., and Moran, M. (1962).—*Nature* **195**: 692.
Mackey, M. B. (1964).—*Proc. Instn. Radio Engrs. Aust.* (in press).
Mills, B. Y., Slee, O. B., and Hill, E. R. (1958).—*Aust. J. Phys.* **11**: 360.
Mills, B. Y., Slee, O. B., and Hill, E. R. (1960).—*Aust. J. Phys.* **13**: 676.
Mills, B. Y., Slee, O. B., and Hill, E. R. (1961).—*Aust. J. Phys.* **14**: 497.
Milne, D. K., and Scheuer, P. A. G. (1964).—*Aust. J. Phys.* **17**: 106.
Ryle, M. (1963).—Report at XIII General Assembly of URSI, Tokyo.